1952

EFFECT OF CURARE ON QUADRICEPS

SHEIN

EFFECT OF CURARE ON INTERRELATIONSHIPS OF FORCE, EMG, JOINT POSITION FOR ISOMETRIC CONTRACTIONS OF QUADRICEPS FEMORIS IN MAN

By

GRAHAM FRASER SHEIN, B.Sc.

A Project
Submitted to the School of Graduate Studies
in Partial Fulfilment of the Requirements
for the Degree
Master of Engineering
McMaster University
October 1980

Master of Engineering (1981)
(Engineering Physics)

MCMASTER UNIVERSITY
Hamilton, Ontario, Canada

Part A

TITLE : Effect of Curare on Interrelationships of Force, EMG, and Joint Position for Isometric Contractions of Quadriceps Femoris in Man

AUTHOR : Graham Fraser Shein, B.Sc.
Queen's University, Kingston,
Ontario, Canada (1978)

SUPERVISOR : Dr. L. D. Pengelly

NUMBER OF PAGES : x; 103

ACKNOWLEDGEMENTS

I would like to gratefully acknowledge the generous support of my advisors, Dr. L.D. Pengelly of the Departments of Engineering Physics and Medicine along with Dr. J.R.A. Rigg and Dr. H. De Bruin, both of the Department of Medicine, who provided me with guidance and expertise in the undertaking of this research project. My thanks are also directed to McMaster University Medical Centre and Chedoke Hospitals for the provision of facilities necessary to this study.

I wish to especially thank the following persons who submitted themselves along with myself to being temporarily partially paralyzed with curare and who provided many stimulating hours of academic discussion concerning this study:

Claudio Gil Soares de Araujo

Fred Buick

Dr. Kieran Killian

Dr. Kees Mauotte

Dr. Alan Menkis

For his assistance in sorting out the statistical problems encountered in handling the vast quantities of data and in detailing how best to make meaningful comparisons of conditions I extend my thanks to Dr. Charles Goldsmith.

Special thanks are extended to Mrs. Liz Inman for her aid as a Research Technician, Miss Ann Popov for her help in typing lists of processed data, and to the Ontario Crippled Children's Centre, Toronto for making available word processing facilities.

ABSTRACT

The interrelationship of force, surface electromyograms (EMG) and joint position for static voluntary contractions of Quadriceps Femoris muscle group in man were investigated before and during partial curarization induced by d-tubocurarine.

Four normal male volunteers were studied. Each performed a series of brief isometric contractions (by extension of the lower leg against resistance) at different levels of force and at three knee-joint positions while lying in the supine position. All series were repeated for both a normal state and a partially paralyzed state under the influence of curare. Torque generated about the knee-joint was measured with a Cybex isokinetic system and the myoelectric activity of three quadriceps muscles was monitored using bipolar surface electrodes.

Traditional parameters of myoelectric activity (mean-rectified-EMG [MRE], and root-mean-squared-EMG [RMSE]) were calculated using a minicomputer (PDP11/34), which had also acquired and processed the data. In addition, EMG power spectra were computed by Fast Fourier Transform techniques in an attempt to provide further insight into the effects of curare on human muscle.

In order to provide a basis for comparison of the normal state with the parially curarized state, force-EMG relationships were computed for each subject, muscle, knee-joint angle, and condition. Statistical methods (three-way ANOVA's) were then employed to both quantify any differences that may have existed between the two states and

to identify sources of differences within each state. A similar statistically-based comparison of the power spectra was undertaken utilizing several indices that described the shape of the spectra. A general description of the activities of the quadriceps femoris muscles followed after collating all the information that the surface EMG provided in conjunction with the external forces measured.

It was concluded that curare did not have any significant effects on the force-EMG relationship. There appeared to be a slight effect of curare on the power spectra however, with a general trend of increasing lower frequency power. The greatest source of variation of force-EMG relationships and power spectra was attributed to the position of the knee-joint.

TABLE OF CONTENTS

LIST OF ILLUSTRATIONS

LIST OF TABLES

CHAPTER I

INTRODUCTION

1.0 Purpose

In recent studies of respiratory mechanics in the Cardio-Respiratory Unit at McMaster University Medical Centre an apparent shift in the diaphragm force-EMG relationship during partial curarization was observed. In attempting to reconcile this observation with current concepts of neuromuscular transmission and block, a paucity of quantitative data was found in the literature. This report presents the results of a systematic study of the interrelationships of force, surface electromyograms (EMG) and joint position for static voluntary contractions of skeletal muscle (Quadriceps Femoris) before and during partial curarization induced by d-tubocurarine.

A comprehensive analysis of the surface EMG signal was undertaken utilizing computer facilities that were made available for this study. The use of the computer enabled, with relative ease, computation of several indices that describe EMG. These included integrated and root-mean-squared-EMG, and also the power spectrum along with its various descriptive indices. Power spectral analyses were included in this study due to their popularity in describing EMG signals, The usefulness and value of this technique was also investigated.

CHAPTER II

METHODS AND MATERIALS

2.0 Introduction

Surface electromyographic (EMG) signals and external force generated by quadriceps femoris muscles were recorded at various levels of voluntary isometric contraction and at different knee-joint positions before and during the infusion of d-tubocurarine (dtc).

This chapter serves as a description of the experimental procedure including the experimental facility, protocol, data collection and data processing.

2.1 Subjects

Four normal male volunteers (ages 22 to 34 years) were studied. See Table 2.1 for a full description of the subjects. All volunteers were aware of the specific effects of the drug and gave informed consent for the study, which was approved by the Human Ethics Committees of both Chedoke Hospitals and McMaster University Medical Centre.

TABLE 2.1 Subject Description

Subject	Age	Height	Weight
F.B.	28	175 cm.	75 kg.
K.K.	30	178	70
K.M.	34	180	82
F.S.	22	180	68

2.2 Experimental Facility

All experiments were performed with the subjects in a supine position on a plinth (padded table) with their lower legs flexed and overhanging the end of the table. Cushions were used to make the subjects as comfortable as possible.

A Cybex II isokinetic system, manufactured by Lumex Inc., was employed to measure the torque generated about the knee-joint resulting from the contraction of the quadriceps. During the experiments, the torque generated was monitored using the built-in scale on the Cybex. In all experiments a precise measurement of torque was obtained by using calibration force levels and processing the Cybex output by computer. The force signal was displayed to each subject using a Tektronix 7613 oscilloscope. A second fixed trace on the oscilloscope served as a force target level for each condition. The Cybex mechanism also included a ring scale with which relative angular movement of the knee-joint was measured.

Three sets of bipolar disposable skin electrodes (Becton-Dickinson, No. 7901) placed over the quadriceps group monitored EMG signals. An indifferent (ground) electrode was placed on the upper leg distant from these muscles.

Small differential preamplifiers, attached to the skin adjacent to the electrodes, were employed to differentially amplify the surface EMG signal by 100. These were coupled between the surface electrodes and the input cable to a PDP11/34 computer. Raw EMG signals were filtered through a 6 Hz., 6 dB/octave as well as a 10 Hz., 24 dB/octave high-pass filter system and amplified by a factor of 10. Cybex torque signals were amplified by a factor of 2 but not filtered.

The EMG signals were acquired on-line by a PDP-11/34 system using a 12-bit analog to digital convertor at a 500 Hz. sample rate, and stored directly on disc in records of 2000 points.

2.3 Calibration

To provide a known torque to the Cybex for calibration purposes, a set weight was placed on the arm of the machine. This arm was allowed to rotate such that the weight moved through an arc passing through a point where the the arm was parallel to the ground and the weight was directed downwards perpendicular to this. At this point the torque was exactly equal to the weight x length of the arm. A zero torque was measured with the arm of the machine in a vertical position.

2.4 Level of Weakness

For the first two subjects, the inspiratory capacity (IC) was measured with a Stead-Wells spirometer before and during the infusion of curare. IC was used as an assessment of dosage knowing that IC should only drop by about 10% for a drop of 50% in skeletal muscle force. For all subjects, the degree of partial neuromuscular block was estimated by comparison of maximum generated torque during the infusion of curare with the control maximum torque as measured by the Cybex.

2.5 Protocol

On the day of the experiment the subject fasted for at least five hours before the experiment. After informing the subject of the sequence of events, the areas of skin for electrode placement were rubbed with an alcohol swab. The three pairs of electrodes were filled with a conductive paste and secured to the skin over the muscles - Vastus Medialis, Vastus Lateralis and Rectus Femoris, as shown in Figure 2.1. An electrode spacing of 3.5 cm. centre to centre was used. The electrode wires were cut short (approx. 15 cm.) and wound tightly together in pairs to reduce noise levels. Each pair of electrode wires was then connected to the preamplifier modules.

Prior to an experiment, signal quality was checked with an UV paper recorder that was integrated with the computer system. At this time any bad electrodes, connections or extraneous noise were identified and eliminated.

Each subject was positioned on the plinth and his lower leg strapped to a padded bar that was part of the Cybex arm assembly. The axis-of-rotation of the arm was centred by eye through the axis of the knee-joint. With the lower leg hanging freely at right angles to the upper leg, the angle position scale was adjusted to read 90°.

2.5.1 Control Session

After calibration of the Cybex the test sequence began. The first series of contractions were maximum efforts with the knee-joint at 90°,

FIGURE 2.1 Quadriceps Muscles and Electrode Placement

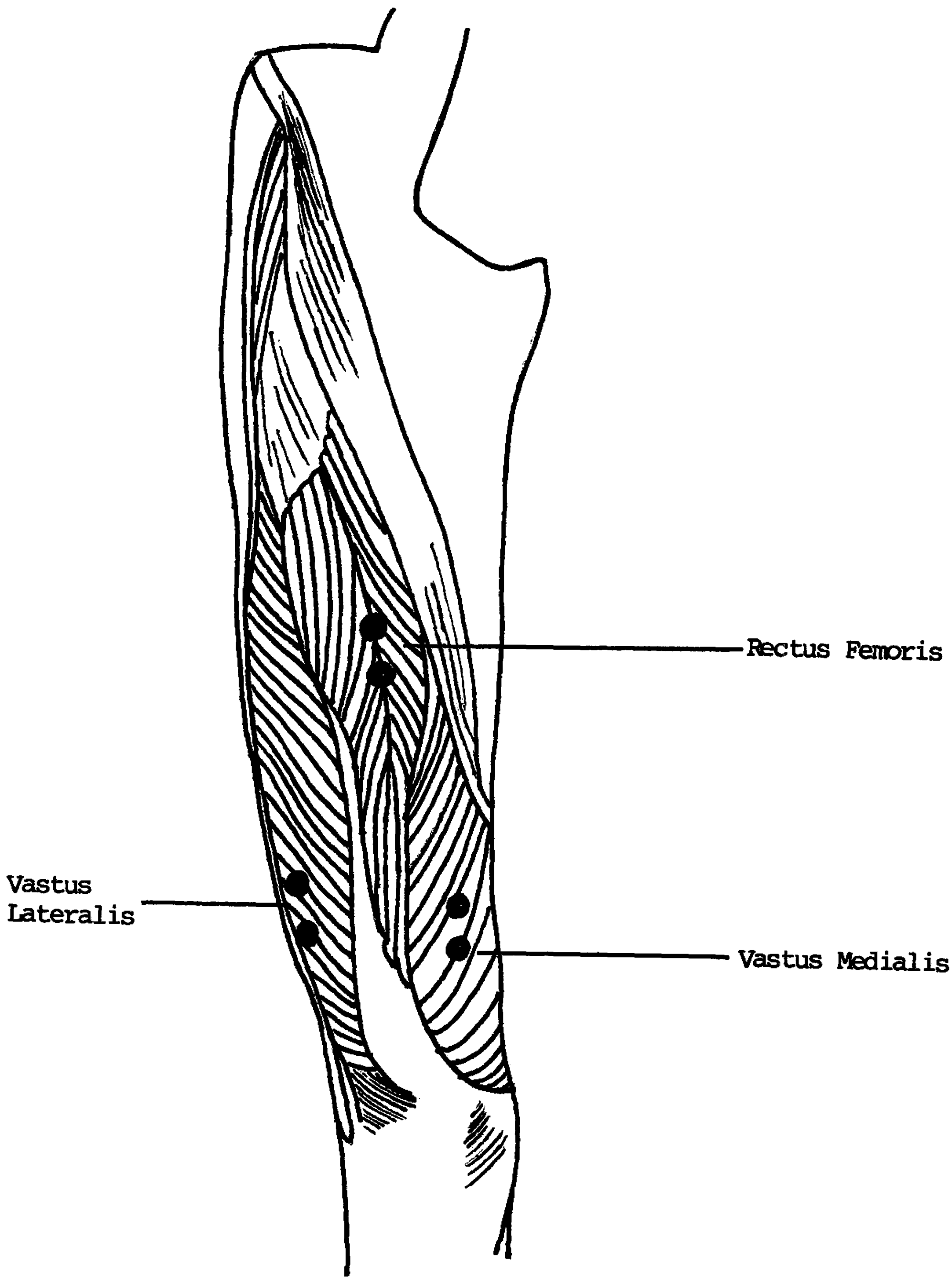

120° and 150° (see Figure 2.2). The second series of contractions were submaximal efforts at each of the three angles where the subject maintained a predetermined (as % of maximum at each angle) force level for at least four seconds using the oscilloscope as feedback. During each contraction, the computer sampled the signals for four seconds.

All contractions were separated by a rest period of at least one minute and were repeated in the order shown in Table 2.2. After completing the sequence of control contractions the subjects rested for a twenty minute period.

2.5.2 Curare Session

Progressive submaximal neuromuscular block (SNMB) to a steady level was induced by intravenous infusion of a dilute solution of dtc with normal saline. The initial rate of infusion was estimated according to the weight of the subject and the known clinical dose-response characteristics of the drug and adjusted during the experiment on the basis of ongoing measurements of maximum leg force and IC. A steady level was maintained throughout with maximum static forces between approximately 50% and 75% of control maximum. As the subject's vision was impaired, he was "coached" by voice to enable maintenance of the desired force. The entire experiment as outlined in Table 2.2 was then repeated for the curarized muscle.

FIGURE 2.2 Knee-Joint Positions

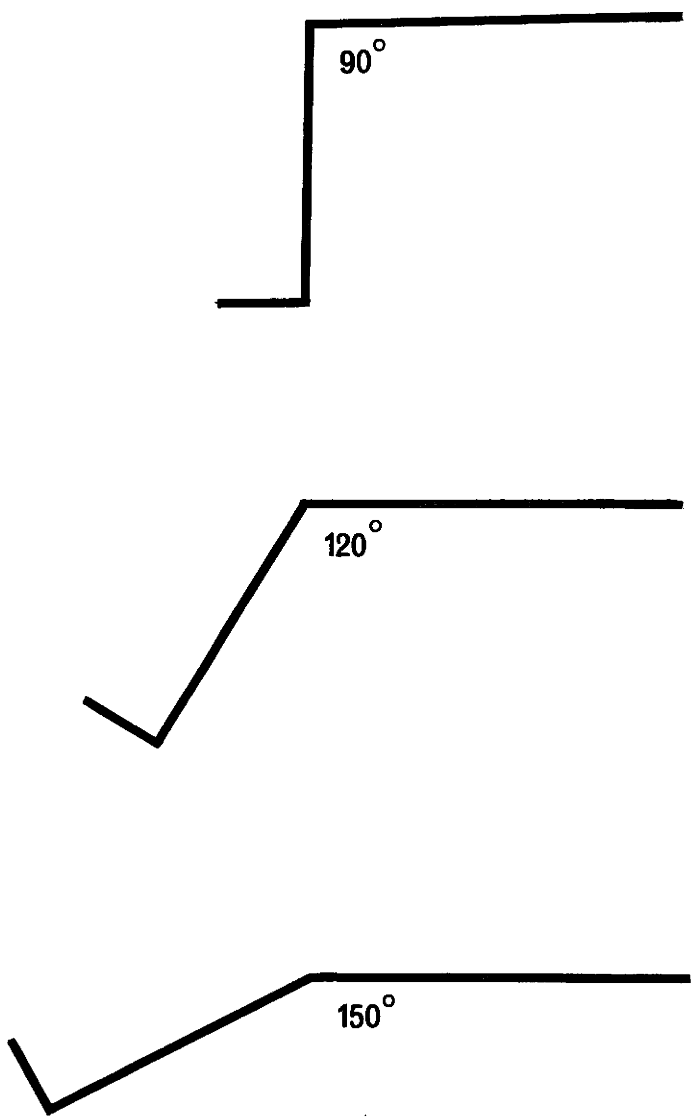

TABLE 2.2 Contraction Sequence

Contraction	Angle	% MVC
1	90°	100
2	120°	100
3	150°	100
4	150°	100
5	120°	100
6	90°	100
7	90°	75
8	90°	50
9	90°	25
10	120°	25
11	120°	50
12	120°	75
13	150°	75
14	150°	50
15	150°	25
16	150°	25
17	150°	50
18	150°	75
19	120°	75
20	120°	50
21	120°	25
22	90°	25
23	90°	50
24	90°	75

2.6 Data Processing

For each contraction, the generated torque, EMG amplitude statistics and EMG power spectra were calculated using computer processing of the acquired data.

From each four-second epoch of data collected, the middle two-second window was analysed rather than the full epoch. Using this middle two seconds of data provided the most steady-state contraction level and hence ensuring stationarity. The precise length of the data window was dictated by the Fast Fourier Transform which required a complex data vector equal in length to a power of two. Therefore, a window of 2048 ms. containing 1024 points was adopted.

A Fortran routine was written to compute the torque measured by the Cybex. This was accomplished by comparing the average of the arithmetically smoothed sample values in the mid-window of each data record containing the Cybex signal, with the calibration records. Torque, T, was calculated as;

$$T = \frac{T_{cal}}{X_m - X_o}(X_s - X_o) \qquad \text{Eq. 2.1}$$

where T_{cal} is the calibration torque, X_m is the smoothed maximum sample value in the calibration record, X_o is the value representing zero torque, and X_s is the unkown torque sample value (smoothed and averaged over the mid-window).

A second Fortran routine was devised to compute several parameters as described below) that were selected to describe the surface EMG signal.

Mean-rectified-EMG (MRE) and root-mean-squared-EMG (RMSE) were calculated over the mid 1024 sample points using the following algorithms;

$$MRE = \frac{\sum_{i=1}^{N} \left|\frac{X_i}{c}\right|}{N} \qquad \text{Eq. 2.2}$$

$$RMSE = \sqrt{\frac{\sum_{i=1}^{N} \left(\frac{X_i}{c}\right)^2}{N}} \qquad \text{Eq. 2.3}$$

where X_i is the sample value in the window of the record being examined that has been corrected for any D.C. offset, N is the number of samples (1024) and c is a constant converting the sample value to unity whenever there is a one microvolt signal.

The power spectra of the EMG signals were calculated using a Fast Fourier Transform (FFT2, International Mathematical and Statistical Library) with a base two algorithm. This particular program utilizes a modification of the Cooley-Tukey FFT algorithm which requires only $n\log_n$ basic sets of operations (Singleton, 1967).

The output of the FFT routine, A(out), is defined as;

$$A(out)_{l+1} = \sum_{j=0}^{n-1} A(in)_{j+1}\, e^{2\pi ijk/n} \qquad \text{Eq. 2.4}$$

where $k=0,1,2,\ldots n-1$; $i=\sqrt{-1}$; $l=r(k)$; $n=2^M$

The function r(k) denotes the reverse binary order in which the coefficients of the output transformed vector are stored. The complex absolute of the coefficients in the output vector are then unshuffled by another library routine to determine the power spectral density function, PSD(f).

The frequency coefficient resolution possible with this technique is the ratio of the sampling rate (500 Hz.) and the number of sample points (1024), which at 0.488 Hz. is sufficient to minimize the effects of 'picket fencing' (Bergland, 1969). Considering the fold-over frequency (or Nyquist frequency) is at coefficient 512 and the resolution is 0.488 Hz., the highest significant frequency in the power spectrum is 250 Hz. Aliasing was negligible because the bandwidth of the signal was less than half the 500 Hz. sampling rate.

Before Fourier transformation, the data were multiplied by a Hanning window (see Appendix 1-A) rather than using a rectangular or 'box-car' window, as was done for the calculation of MRE and RMSE. A Hanning window resembles a cosine bell on a pedestal and has been shown to reduce leakage into the side lobes. This leakage is an inherent problem with any Fourier analysis of finite length (Bergland, 1969, Blackman-Tukey, 1958, Brigham, 1974).

The total power, PWR, of the spectrum was determined by the integration of the PSD(f) over the bandwidth from 15 Hz. to 250 Hz. as follows;

$$PWR = \sum_{f=15}^{250} PSD(f) \qquad \text{Eq. 2.5}$$

where T is the period of the data window in seconds, and f is a frequency in the spectrum.

Per cent power (%PWR) with respect to total PWR in three bandwidths, 15-50 Hz., 50.3-124.5 Hz. and 125-250 Hz. was calculated by similar technique. A high/low (H/L) ratio of the %power in the high band divided by the %power in the low band was also obtained.

Centroid frequency, f_c, was determined by the relationship;

$$f_c = \frac{\sum_{f=15}^{250} f \times PSD(f)}{\sum_{f=15}^{250} PSD(f)} \qquad \text{Eq. 2.6}$$

where f, as before, is a frequency in the spectrum.

Band %PWR, H/L ratio and f_c indicated and quantified the EMG frequency distribution and provided a basis for quantitative assessment of any frequency shift in the spectrum. These indices are also those standardly employed to describe EMG spectra although the bands may be different than used by others.

CHAPTER III

RESULTS

3.0 Force Levels

Subjects received a total dose of dtc which averaged 17 ± 1 mg. (mean ± S.D.). However, due to the nature of the drug, each subject reached different relative levels of muscular weakness. The loss in force developed by each individual is illustrated in Figure 3.1 where average maximum voluntary contractions (MVC) as per cent of MVC at 90° are plotted against knee-joint angle. The lowest force developed at 90° with curare was 44% MVC in subject F.B. and the highest level was 80% MVC in subject K.M..

As reported previously (Haffajee et al, 1972, Rigg, 1978), maximum torque output of the quadriceps group decreased with increasing knee-joint angle. Similar results were observed in this study under the effects of curare but at reduced maximum torque levels. These reductions in torque levels appeared to vary at each angle with a greater average reduction in force (45%) at 150° than 90° (36%).

FIGURE 3.1 Average Maximum Voluntary Isometric Contractions vs. Knee-Joint Angle

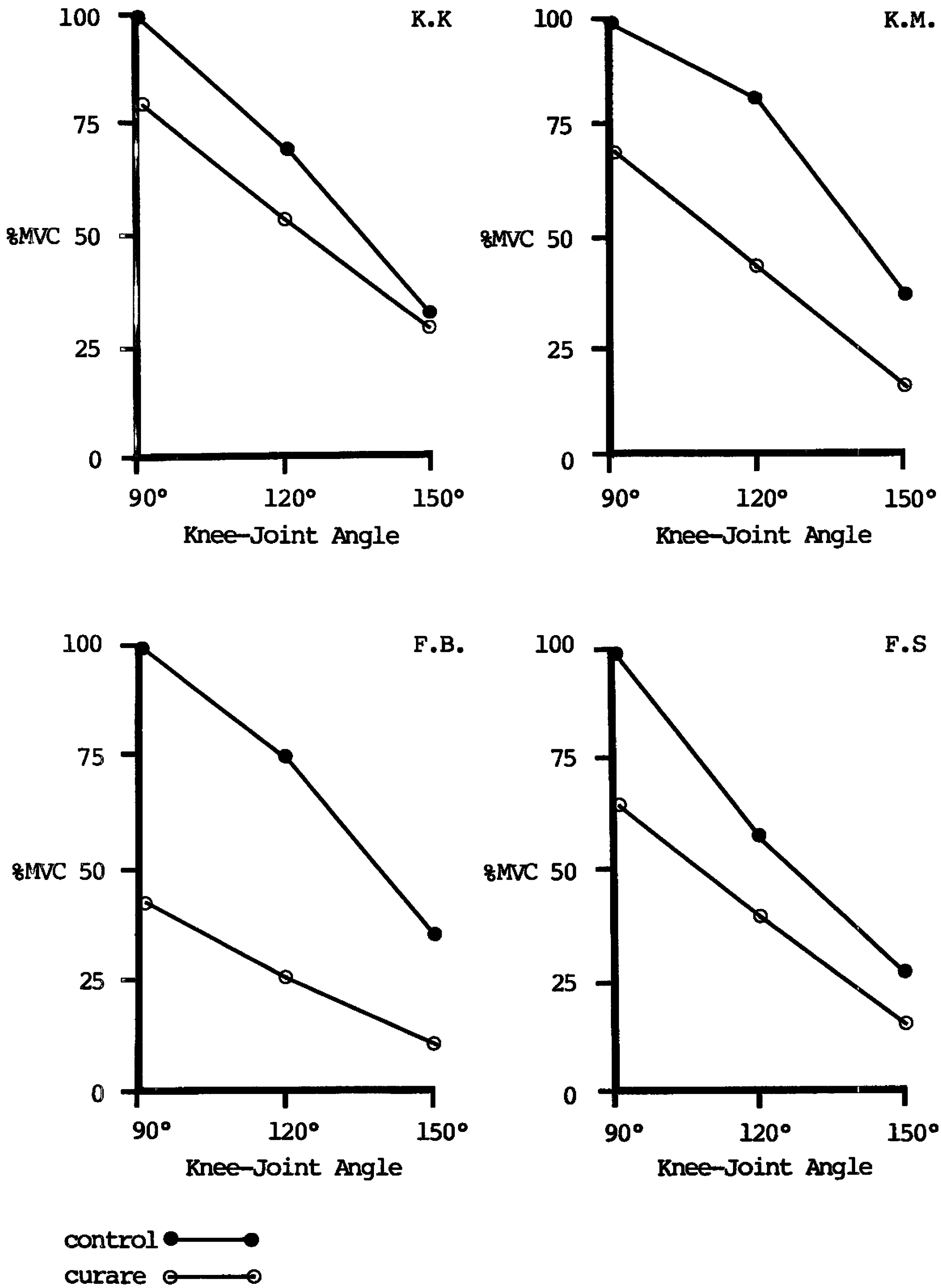

3.1 Torque-MRE relationship

As shown in Figures 3.2 and 3.3 a definite relationship exists between torque and mean-rectified-EMG (MRE) for a single subject, muscle, knee-joint position and condition. It is clear that an increase in MRE results in an increase in torque output of the muscles involved.

Previously, force-EMG relationships had been described as being both linear (Milner-Brown, 1975) and non-linear (Zuniga, 1969, DeLuca, 1979). With this in mind, both linear and quadratic regression analyses were employed (see Appendix 1-B) to fit mathematical relationships to torque-MRE data. As there was no physiological basis for assuming otherwise, both regressions were designed to force the fitted line/curve through the zero origin. This implies that there is no torque developed when electrical activity is absent. Other regression techniques (power, exponential, logarithmic, and least squares) were attempted but dismissed as unsatisfactory and misleading.

Tables 3.1 - 3.4 list values for the regression coefficients B, B_1, and B_2 of the following equations that were derived for the data:

$$MRE = B \times T \qquad \text{Eq. 3.1}$$

$$MRE = B_1 \times T + B_2 \times T^2 \qquad \text{Eq. 3.2}$$

where T is torque and the equations are applicable to a single subject, muscle, knee-joint angle and condition. As well, coefficients of determination (uncorrected for the mean) which describe the goodness of

FIGURE 3.2 Torque-MRE Linear Relationships: Control and Curare Conditions; Subject K.K.; Vastus Medialis; @90°

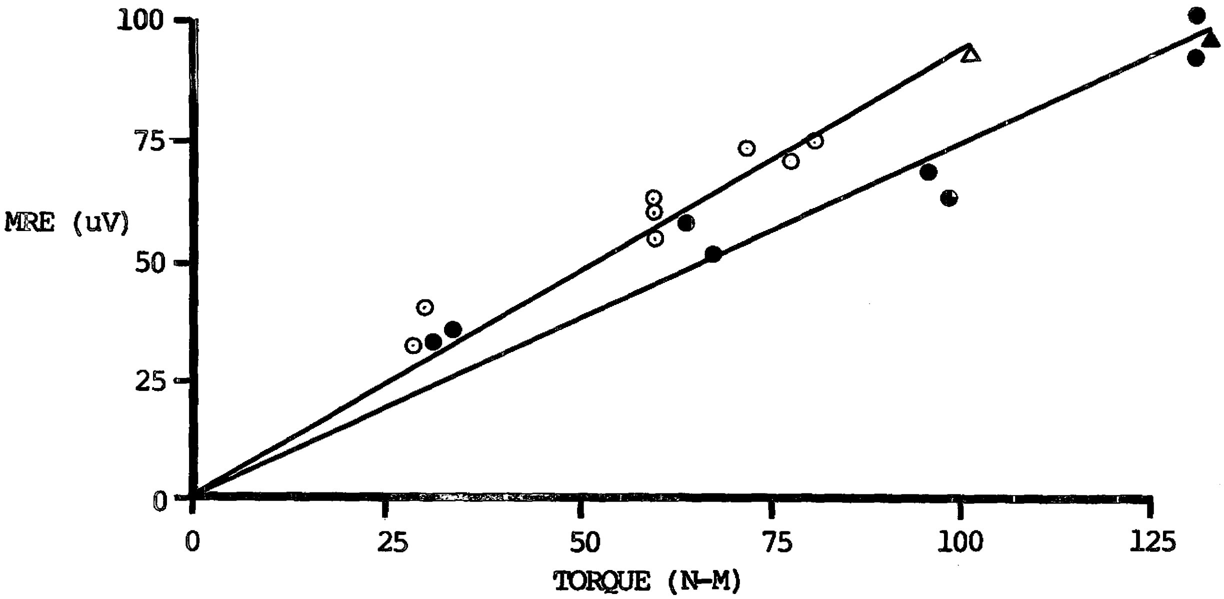

FIGURE 3.3 Torque-MRE Quadratic Relationships: Control and Curare Conditions; Subject K.K., Vastus Medialis; @90°

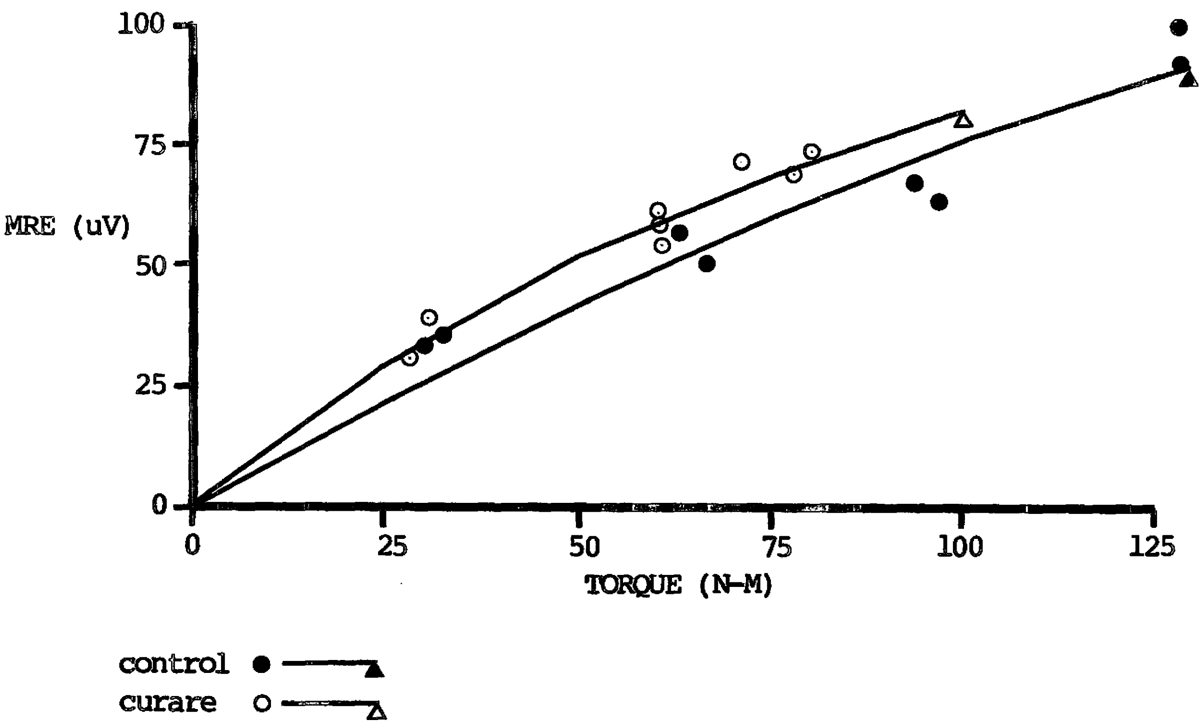

TABLE 3.1 Linear Torque-MRE Relationship: Control Condition

Muscle	Subject	KNEE-JOINT ANGLE					
		90°		120°		150°	
		B*	r^2**	B *	r^2*	B*	r^2**
Vastus Med.	K.K.	0.74	0.99	1.33	0.98	4.08	0.97
	K.M.	0.75	0.99	0.87	0.98	1.78	0.97
	F.B	0.68	1.00	0.97	0.99	1.98	1.00
	F.S.	1.02	0.98	1.55	0.98	2.92	0.99
Vastus Lat.	K.K.	0.96	0.99	1.51	0.98	4.40	0.98
	K.M.	0.82	1.00	1.06	0.98	2.32	0.97
	F.B.	1.76	0.96	3.34	0.98	7.15	0.99
	F.S.	0.98	0.97	2.07	0.99	4.16	0.99
Rectus Fem.	K.K.	0.90	0.95	2.16	0.97	4.11	0.99
	K.M.	0.71	0.98	1.12	0.97	2.70	0.98
	F.B.	1.21	0.99	1.21	0.99	2.21	0.99

* MRE = B x Torque

** coefficient of determination uncorrected for the mean

TABLE 3.2 Linear Torque-MRE Relationship: Curare Condition

Muscle	Subject	KNEE-JOINT ANGLE					
		90°		120°		150°	
		B*	r^2**	B*	r^2**	B*	r^2**
Vastus Med.	K.K.	0.93	1.00	1.08	0.99	3.25	0.97
	K.M.	0.77	0.97	0.88	0.96	2.16	0.96
	F.B	0.87	0.96	1.02	0.97	3.62	0.99
	F.S.	1.26	0.97	2.27	0.93	5.30	0.98
Vastus Lat.	K.K.	1.20	0.99	1.33	0.98	3.17	0.97
	K.M.	0.86	0.99	1.14	0.96	2.61	0.96
	F.B.	1.22	0.98	1.62	0.98	4.45	0.99
	F.S.	0.97	0.98	2.36	0.93	5.99	0.98
Rectus Fem.	K.K.	0.70	0.97	0.88	0.96	2.09	0.97
	K.M.	0.55	0.94	0.74	0.97	1.83	0.99
	F.B.	1.47	0.97	1.25	0.97	3.10	0.99

* MRE = B x Torque

** coefficient of determination uncorrected for the mean

TABLE 3.3 Quadratic Torque-MRE Relationship: Control Condition

Muscle	Subject	KNEE-JOINT ANGLE								
		90°			120°			150°		
		B_1*	B_2*	r^2**	B_1*	B_2*	r^2**	B_1*	B_2*	r^2**
Vastus Med.	K.K.	0.87	-0.001	0.99	1.21	0.001	0.98	5.79	-0.430	0.98
	K.M.	0.80	0	0.99	0.55	0.003	0.99	2.63	-0.020	0.99
	F.B.	0.62	0	1.00	0.45	0.004	1.00	1.20	0	1.00
	F.S	0.68	0.002	0.98	0.48	0.009	0.99	4.30	-0.024	1.00
Vastus Lat.	K.K.	0.89	0.001	0.99	1.33	0.002	0.98	6.23	-0.046	0.99
	K.M.	0.69	0.001	1.00	0.60	0.004	0.99	3.60	-0.030	0.99
	F.B.	2.29	-0.003	0.96	2.13	0.009	0.98	10.08	-0.044	0.99
	F.S.	0.40	0.003	0.99	1.02	0.009	1.00	6.14	-0.033	1.00
Rectus Fem.	K.K.	0.22	0.006	0.99	1.10	0.012	0.98	4.39	-0.007	0.99
	K.M.	0.42	0.002	1.00	0.49	0.006	1.00	3.66	-0.022	0.99
	F.B.	1.13	0	0.99	0.77	0.003	1.00	2.94	-0.011	1.00

* $MRE = B_1 \times Torque + B_2 \times (Torque)^2$

** coefficient of determination uncorrected for the mean

TABLE 3.4 Quadratic Torque-MRE Relationship: Curare Condition

Muscle	Subject	KNEE-JOINT ANGLE								
		90°			120°			150°		
		B_1*	B_2*	r^2**	B_1*	B_2*	r^2**	B_1*	B_2*	r^2**
Vastus Med.	K.K.	1.16	-0.003	1.00	1.27	-0.003	0.99	6.07	-0.121	0.99
	K.M.	0.88	-0.001	0.97	1.04	-0.002	0.96	3.08	-0.021	0.98
	F.B.	0.83	0.001	0.96	0.36	0.012	0.99	5.50	-0.087	0.99
	F.S	0.81	0.004	0.98	2.27	0	0.93	6.38	-0.034	0.99
Vastus Lat.	K.K.	1.15	0.001	0.99	1.19	0.002	0.98	5.16	-0.086	0.99
	K.M.	0.68	0.002	0.99	0.94	0.002	0.96	3.64	-0.023	0.98
	F.B.	0.91	0.004	0.98	1.04	0.010	0.98	4.77	-0.015	1.00
	F.S.	0.79	0.015	0.98	2.02	0.005	0.93	7.84	-0.058	0.99
Rectus Fem.	K.K.	0.27	0.006	0.98	1.10	0.012	0.99	3.16	-0.046	0.98
	K.M.	0.03	0.004	0.99	0.27	0.006	0.99	1.84	0	0.99
	F.B.	1.60	-0.002	0.97	0.51	0.013	0.98	2.22	0.041	0.99

* $MRE = B_1 \times Torque + B_2 \times (Torque)^2$

** coefficient of determination uncorrected for the mean

fit of the relation to the data are listed (see Appendix 1-B). This relationship is slightly better described as a quadratic (average r^2 = 0.99 for a quadratic and average r^2 = 0.98 for a linear fit in the control condition).

Examination of Tables 3.1 -3.4 reveals a great deal of variation in the torque-MRE relation. Alterations in the knee-joint position had the most significant effect. As the angle increased, the slope of the relationship consistently increased. This meant a reduction in torque for a constant level of myoelectric activity.

A three-way analysis of variance (ANOVA, $P<0.05$)(see Appendix 1-C) was applied to the data for each of the three muscles and for both methods of regression. The sources of differences tested included - subjects; knee-joint angles; and conditions. F-values due to each source are given in Table 3.5 together with their significance.

Similar conclusions may be drawn from both linear and quadratic analyses. Knee-joint angle had the greatest effect on the torque-MRE relationships. To a much lesser extent, subject differences contributed significantly to some results, while curare did not significantly affect the relations at all.

For a more precise illustration of the variation in the torque-MRE relation with varying knee-joint angle, the linear regression coefficients were corrected (see Appendix 1-C) for subject and condition differences, and then averaged at each angle. These averages were used to calculate torque at a constant level of activity (MRE = 100 uV) and

TABLE 3.5 F-Values Due to Various Sources Affecting both Linear and Quadratic Torque-MRE Relationships

Muscle	Source					
	Subject		Knee-Joint Angle		Condition	
	Lin.	Quad.	Lin.	Quad.	Lin.	Quad.
Vastus Med.	4.27*	3.19	32.2*	34.6*	2.56	1.90
Vastus Lat.	5.02*	2.98	30.9*	21.8*	0.75	1.12
Rectus Fem.	1.68	1.93	17.5*	24.7*	2.57	1.61

* significant @ $P<0.05$

plotted in Figure 3.4. A consistent reduction in torque was observed as the joint angle increased. Vastus Lateralis displayed a relatively constant reduction in torque through the range of angles investigated. Vastus Medialis and Rectus Femoris demonstrated a greater decrement in torque between 120° and 150° than between 90° and 120°.

3.2 Torque-RMSE Relationship

The relationship between torque and root-mean-squared-EMG (RMSE) was not fully investigated as RMSE values were found to be linearly proportional to MRE values as anticipated and predicted by Milner-Brown (1975), and Stulen and DeLuca (1978).

Computations using MRE and RMSE values over one hundred contractions showed that:

$$MRE = 0.753 \times RMSE \qquad r^2 = 0.999 \qquad \text{Eq. 3.3}$$

Therefore, further calculations using RMSE would not yield any additional information pertinent to this investigation.

3.3 Spectral Analysis

3.3.1 Torque-Total PWR Relationship

Total power as derived from spectral analysis of EMG signal (see Figure 3.4) indicated the level of myoelectric activity of a muscle in much the same manner as amplitude statistics such as MRE and RMSE. As

FIGURE 3.4 Estimated Torque Levels for Three Quadriceps Muscles (V.M., V.L.,& R.F.) at a Constant Level of MRE (100 uV) Corrected for Subject and Condition Differences vs. Knee-Joint Angle

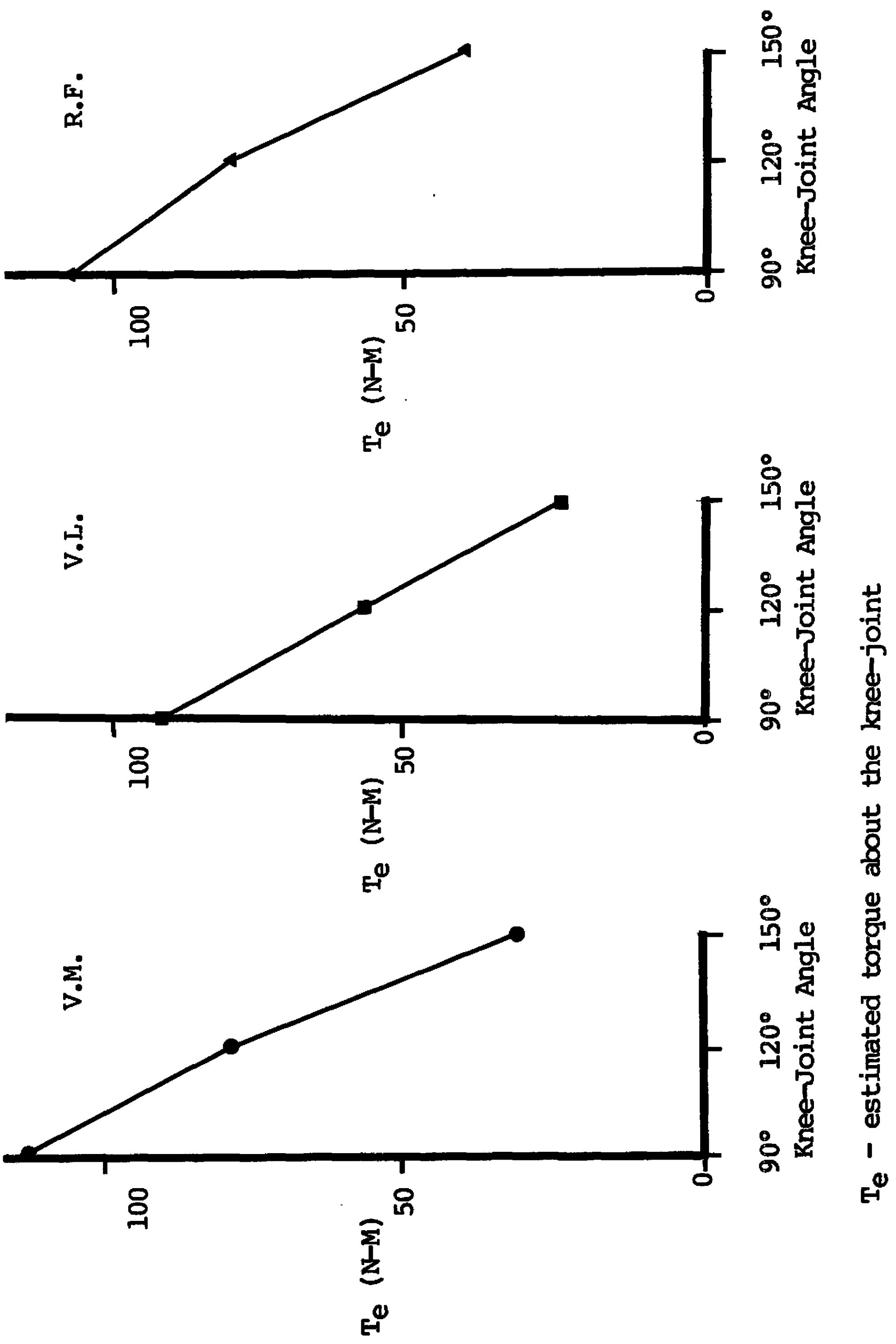

power varies with the square of voltage, PWR is a much more sensitive index. A direct relation between PWR and MRE was found for the data and is:

$$MRE = 3.51 \times \sqrt{PWR} \qquad r^2 = 0.997 \qquad \text{Eq. 3.4}$$

The same variations, or lack of, occurred in torque-PWR relations as with torque-MRE relations with regard to subject, muscle, knee-joint angle and condition differences because of the above mentioned proportionality. Further analyses using PWR were therefore unwarranted. However, the strong correlation between MRE and PWR does confirm the validity of the statistical calculation algorithms (programs).

3.3.2 Power Spectra

No apparent correlation existed between levels of contraction and the spectrum shapes. Linear regressions of MRE versus f_c for each subject, muscle, joint angle, and condition showed no patterns of slope being anything other than essentially zero. This implied that fc was independent of force levels. Assuming that this observation was valid and could be extended to the spectrum as a whole, further calculations used averaged spectrum indices at all levels of force. Variations in each index were calculated but neglected in further computations. Centroid frequencies had an average standard deviation of 6% of their mean values. In comparison, %PWR in each band and H/L ratios had average standard deviations of 15% and 34% respectively.

Differences in the each index due to subject, joint-angle, and condition variations were tested for significance using three-way

```
FILE: SHEIN1.DAT        RECORD NO.  14
WINDOW FROM 1.0 SEC. TO 3.0 SEC.        MULT: 50

FREQ. BANDS:          15 -  50        50 - 125        125 - 250
% POWER IN BAND:        30.              49.              20.

TOTAL POWER IN  250 HZ. BAND= 0.126E 05
THE MEDIAN FREQ. IS  83 HZ.
THE H/L RATIO IS 0.675 FOR BANDS  15- 50  125-250
THE MRE IS=0.211E 00 MV
THE RMS EMG IS=0.272E 00 MV
```

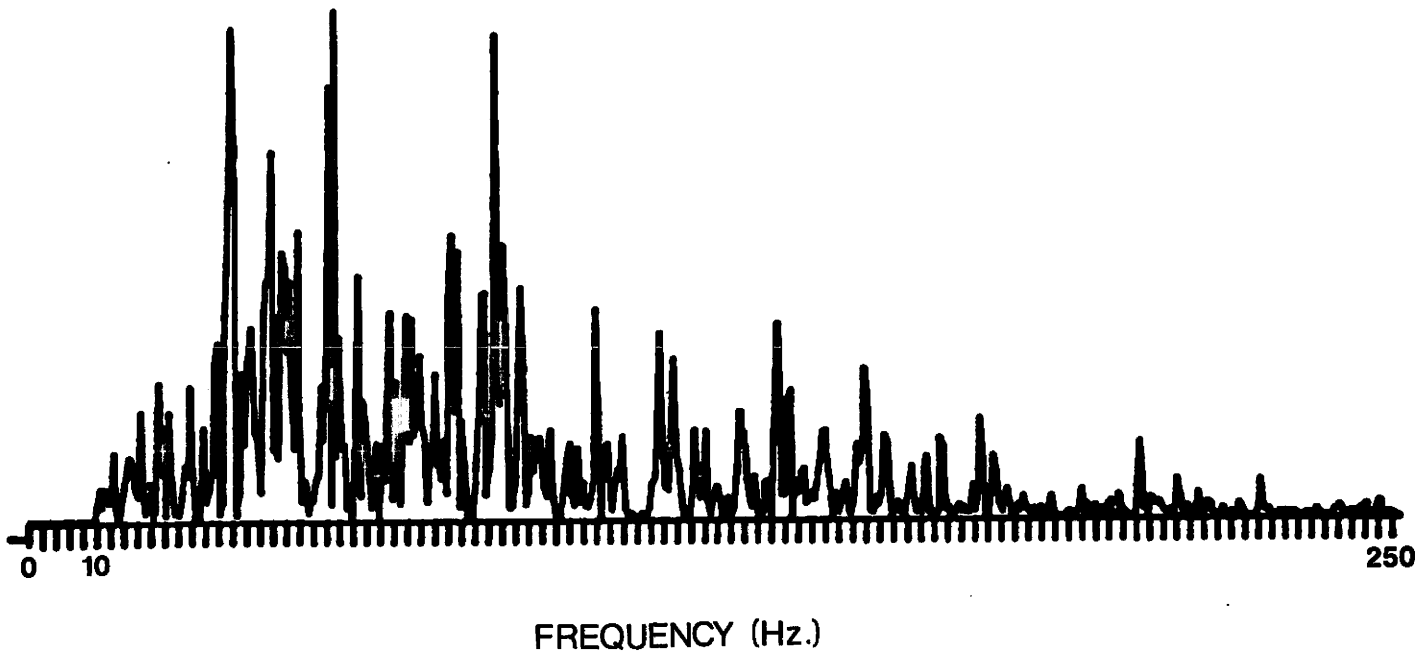

FIGURE 3.5 Typical EMG Power Spectrum

ANOVA's ($p<0.05$) for each of the quadriceps muscles studied. The results are presented in Tables 3.6 a, b, c (see Appendix 1-D). Significant spectral shifts due to subject variances were pronounced but less than those resulting from changing knee-joint angle. Curare did not have a statistically significant effect on the spectra except with Rectus Femoris, although a general trend of higher percentage of power in lower frequencies was evident in all muscles with curare. This decrease in percentage of high frequency power with curare, as well as the rise in frequency attributed to increasing joint angle, is best illustrated in terms of f_c as in Figure 3.6. In this figure the f_c values have been corrected for any subject differences.

Muscle	Index				
	fc	L-Band	M-Band	H-Band	H/L
Vastus Med.	4.28*	9.88*	5.30*	3.04	7.90*
Vastus Lat.	8.39*	2.32	23.1*	18.8*	6.54*
Rectus Fem.	0.19	6.09*	9.16*	0.05	0.15

* significant @ P<0.05

Table 3.6 a) F-Values with Subject as Source Affecting Power Spectrum

Muscle	Index				
	fc	L-Band	M-Band	H-Band	H/L
Vastus Med.	22.5*	13.7*	0.62	17.3*	17.3*
Vastus Lat.	26.6*	28.8*	4.50*	23.6*	19.0*
Rectus Fem.	20.6*	34.4*	2.38*	12.7*	14.7*

* significant @ P<0.05

TABLE 3.6 b) F-Values with Knee-joint Angle as Source Affecting Power Spectrum

Muscle	Index				
	fc	L-Band	M-Band	H-Band	H/L
Vastus Med.	1.18	0	1.10	1.53	1.48
Vastus Lat.	3.76	11.2*	7.04*	2.33	4.33*
Rectus Fem.	6.45*	6.24*	0.58	5.44*	5.94*

* significant @ P<0.05

TABLE 3.6 c) F-Values with Condition as Source Affecting Power Spectrum

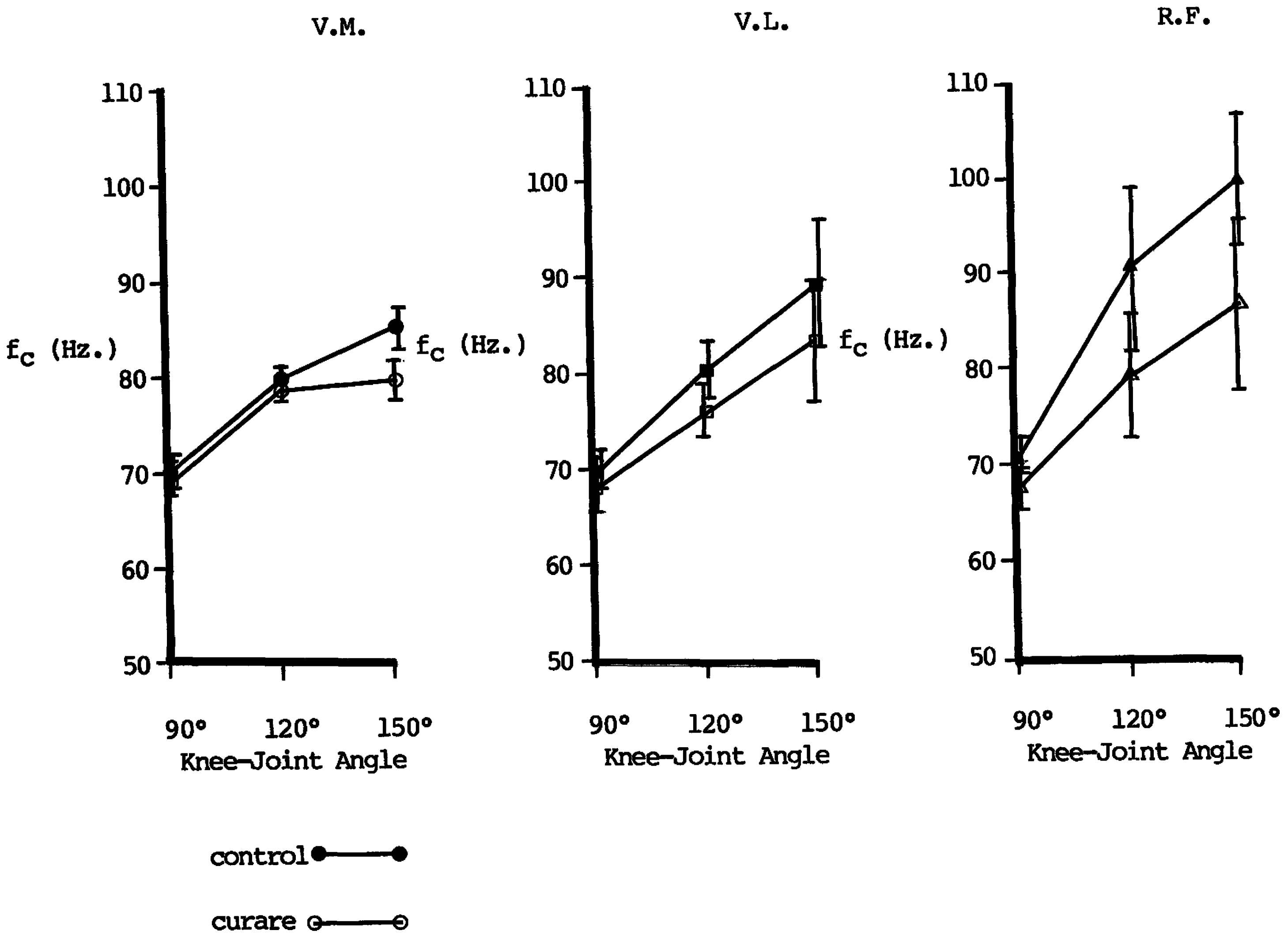

FIGURE 3.6 Centroid Frequency, fc, vs. Knee-Joint Angle for Three Quadriceps Muscles (V.M., V.L.,& R.F.) Corrected for Subject Differences

CHAPTER IV

DISCUSSION

4.0 Introduction

The results of these experiments demonstrate the interrelations between force, EMG and joint position with the human quadriceps muscles in a normal and partially curarized state. These factors were systematically studied for approximately two hundred contractions with four subjects and are discussed in detail in this chapter.

4.1 Action of Curare

The actions of curare have been well documented with respect to its post-synaptic action and only recently (Glavinovic, 1979) has evidence of pre-synaptic action been demonstrated. Curare produces its greatest effect as a competitor with acetylcholine for specific motor end-plate receptors at the neuromuscular junction. Its effect is randomly distributed in such a way that some end-plates are affected while others are not at any given moment. Acetylcholine is still released from the axon terminal but the probability of successful synaptic transmission and subsequent development of an end-plate-potential is reduced depending upon the concentration of curare. There will be some concentration of curare however, that the end-plate will be blocked entirely and will be totally unresponsive to acetylcholine for some period of time. At that point that muscle fibre becomes oblivious to any neural signals.

With submaximal neuromuscular blockade (SNMB) the neural frequency is not transmitted directly into muscle firing frequency as would happen in the normal state, but is reduced relative to the dosage of curare. In this way, the effect of curare can be said to mimic the action of submaximal stimulation. If some fibres are blocked entirely, than those fibres are removed from active participation of developing force in parallel with other fibres. At the present time it is difficult to realize all mechanisms involved in SNMB with curare in humans due to measurement difficulties. Therefore, it is not yet known what proportion of fibres are entirely blocked by the action of curare and what proportion of fibres have reduced firing frequencies, or even whether entire motor units are affected separately.

Curare has a lesser effect on the pre-synaptic side of the neuromuscular junction. Recently, Glavinovic (1979) has shown some evidence of significant action here. He postulated that curare blocks pre-synaptic action of acetylcholine, thereby reducing Ca^{++} permeability and its subsequent influx which is associated with depolarization of the axon terminal. As a result, the responses in the terminal (ie. release of acetylcholine) are depressed.

4.2 Maximum Tension-Angle Relationships

An observed reduction in maximum torque generated about the knee-joint with increasing joint angle is consistent with previous observations (Rigg, 1978). This action follows as a result of varying mechanical action and muscle length.

The axis-of-rotation of the knee-joint is not fixed as in a hinge but rather moves throughout the range of motion. As well, the patella shifts depending upon the position of the knee-joint. These factors alter the lever of the quadriceps (ie. perpendicular distance of the force resultant in the quadriceps tendon from the chosen axis) and consequently vary the torque developed. However, according to Lindahl and Movin (1967) this variation in lever length is only approximately 25 per cent between 90° and 170°. In this study, the variation in torque between 90° and 150° averaged about 70 per cent. The greater variation in torque cannot therefore simply be accounted for by a mechanical alteration of the quadriceps lever.

Although care was taken to ensure that the torque developed was only a result of knee extension, hip flexion may have contributed to the torque. This was most likely at higher angles and may have lead to an overestimate of torque. In addition, extra effort is required to lift the lower limb against gravity as knee-angle increases. Calculations did not include these opposing actions as the experimental set-up did not include means of objectifying them.

The maximum force that the quadriceps are capable of generating depends also upon muscle length. Classical force-length descriptions of skeletal muscle express maximum tension, for constant myoelectric activity, as developed at resting length and decreasing as muscle either shortens or lengthens. Clarke et al (1949) described the optimal position of muscle function to be when tension is optimal but not necessarily maximal and when the angle of pull provides for the greatest leverage.

In the case of increasing knee-joint angle as in this study, the quadriceps shortened thereby reducing maximum force output. However, there were no measurements (for technical reasons) of changes in length of the quadriceps and therefore no means of knowing the contribution each muscle made to the variation of torque.

There are several other factors contributing to variation in maximum torque output. (1) The degree of shortening for each of the muscles studied is dependent upon the alignment of fibres and according to the attachment and insertion points. (2) As the knee-joint changes position the mechanical advantage of the muscle fibres too must also change. (3) Some of the fibres of the quadriceps run obliquely while others do not and (4) total fibre length varies also. A simple description of variation in length and the corresponding force output is therefore quite difficult. For this reason force was plotted against knee-joint angle and not correlated directly to quadriceps length.

Maximum static force-angle relationships under the effects of SNMB with curare are similar to those found previously by Pengelly and Rigg (1978). They concluded that SNMB with curare affects the tension-length characteristic of tibialis anterior of the cat in much the same way as submaximal stimulation. Studies by Rack and Westbury (1969) established that muscle length affects tension differently at different stimulus rates. Furthermore, stimulus rate has a different affect on tension at different muscle lengths. Therefore, a decrement in force with curare would be expected at all joint positions but this reduction should not necessarily be by the same proportion at all positions. Assuming the same maximum effort at each angle, under the effects of curare it should be increasingly more difficult as joint angle increases to reach the same proportion of control maximum as the proportion at 90° when the quadriceps are longer.

In this study, the reduction in torque varied somewhat between each angle with an average reduction of 45 per cent at 150° and 36 per cent at 90°. However, more calculations should be done before any conclusions are drawn with regard to specific proportionality of reduction in force at each angle with curare.

4.3 Amplitude Statistics

Mean-rectified-EMG (MRE) and root-mean-squared-EMG (RMSE) were chosen as being standard measures of EMG amplitude. In the past, there has been some discrepancy among researchers regarding the techniques of measuring EMG amplitude and what name to apply to the value measured. However, all methods are functionally similar, ie. rectified or root-mean-squared-EMG is integrated over some finite period of time. The integration of EMG signal is usually done through an electronic 'black box' where the output is dependent upon some time constant (resistance x capacitance) inherent to the 'box'.

MRE and RMSE were digitally computed in this study over the middle two seconds of four seconds of data collected during a contraction. This digital technique allowed the calculation of the true average EMG amplitude rather than an electronic integration. As discussed before, a mid-window analysis also ensured stationarity and best approximated the activity during the contraction. Fatigue was assumed not to have any effect and indeed there was no evidence to suggest that fatigue influenced the results.

Relationships between force and EMG have been investigated thoroughly in the past and muscle activity or muscle force can now be defined in terms of EMG activity. However, even today there is not total agreement regarding the force-EMG relationship. Both linear and non-linear relationships have been hypothesized for isometric contractions in previous studies.

To ensure that either a linear or non-linear relationship did not conceal information that the other one might disclose, both linear and quadratic analyses were performed on the torque-MRE data. A few subtle differences were seen between the results but both indicated the same variations that occurred in the force-EMG relations. In most cases the quadratic relationship was really quite linear and had only a slightly higher coefficient of determination. The fact that torque rather than force was used does not influence the force-EMG relation as the lever arm of the Cybex remained constant. The torque was then analogous to force.

Considering all the highly complex physiological events that occur within muscle structure during contraction, and considering the visco-elastic properties of muscle tissue, a purely linear force-EMG relationship is unlikely over the entire force range. However, for practical purposes, a linear fit yields a satisfactory approximation to the real situation with isometric contractions, providing that joint position and electrode placement remains constant.

The results of this study clearly show that with isometric contractions, joint position might be the greatest source of variation in any force-EMG relationship. As the knee-joint increased from 90° to 150°, the torque-MRE relationship always increased for both control and curare conditions. Testing these shifts with three-way ANOVAs showed a high degree of significance in every case. The increase in slope implies that torque output decreases for a constant level of EMG as the knee extends.

There are a number of factors that can account for the variations just mentioned. Most of the variation can be explained by considering the force-length characteristics of muscle and the varying mechanical advantages of the knee-joint and patellar tendon. Other factors include - alteration in motor unit recruitment; changing muscle bulk; movement of electrodes with respect to underlying muscle fibres; and variation in skin and fascia thickness. At the present it is not known to what extent each of these other factors affect the EMG signal and whether all their effects are significant in this study. First, variation in motor unit recruitment is likely at different positions of the knee as the recruitment order is stable only for given movement task (Person,1974). As the knee-joint changes position the muscle task will change and so the recruitment pattern may also vary. Second, an increase in muscle bulk as muscle shortens brings more fibres under the electrodes. This increases the quantity of EMG signal monitored. Third, the muscle shifts by some degree under the layer of skin and fascia. Therefore, the electrodes that are stationary on the skin, may overlie an entirely different section of muscle fibres at knee-extension compared with knee-flexion. This factor is most significant when the electrodes are placed over oblique fibres, as occur in parts of the quadriceps, because the electrical activity may vary across fibres. When the electrodes are overlying longitudinal fibres, muscle shift is not as significant a factor since the EMG does not vary along the fibre unless the cross-sectional area changes. Last, a very slight change in surface layer thickness can have a very pronounced effect on signal power (Lynn et al, 1978).

Milner-Brown et al (1975) and DeLuca (1978) demonstrated the linear relation between MRE and RMSE. They computed the relationship theoretically assuming the distribution of voltages from overlapping independent motor units to approach a Gaussian distribution in accordance to the Central Limit Thereom (Cox and Miller, 1965). With this assumption and also the fact that MRE varies at some rate r, while RMSE increases as the square root of r, the following equation was derived:

$$MRE = \sqrt{\frac{2}{\pi}} = 0.798 \times RMSE \qquad \text{Eq. 4.1}$$

However, this approximation is only correct if the number of units remains constant and an increase in firing rate is the sole factor in increasing force. This situation is unlikely over the entire range of force.

At initial recruitment, firing rate is relatively unstable and up to about 30% MVC recruitment plays the dominant role with the smaller units being recruited first (Henneman et al, 1965). Progressively larger units are recruited in an orderly fashion (Milner-Brown et al, 1973a), and at the same time firing rate increases but at a slower rate (Milner-Brown, 1973b). Between 30% and 75% MVC, recruitment of larger units occurs but is secondary to increases in firing rate. Above 75% MVC recruitment in most muscles essentially ceases while increases in firing rate continue.

In this study, the relation between MRE and RMSE was shown to be highly linear. The proportionality constant was 0.753 with a coefficient of determination of 0.999 (N=100). As this constant was calculated above 25% MVC it is possible that very little recruitment occurred and the increase in force was due in most part to increases in firing rate.

An increase in the slope of the force-EMG relationship during SNMB with curare was expected as it was previously observed (Pengelly and Rigg, 1979). Also, the action was likened to that observed with a fatigued or myopathic muscle which has been shown to exhibit such a shift. Although this shift was seen in some cases, there were as many cases where it occurred in the opposite direction. Statistical analyses indicated that in fact there were no significant effects of curare on the force-EMG relations. This is not an unreasonable conclusion with surface electrodes even though it is contrary to past observations. Normal integrative techniques of examining surface EMG cannot distinguish between the activity of a normal muscle and a partially curarized muscle where more units are active but fire at slower rates. The sum total of each of the two states will appear to be the same.

4.4 Spectral Analysis

Power spectra of the EMG signals calculated by FFT techniques provide a further insight into myoelectric activity by comprehensive analysis of the signal, but cannot by themselves clarify the mechanisms involved. However, due to the great interest in spectral analysis held by many researchers and in the hope of explaining some discrepancy with past research by Pengelley and Rigg (1979) it was decided to include this technique in this study.

A power spectrum is simply the collection of separate frequency components that comprise an electric signal. To enable comparisons of different spectra various indices are employed. Total PWR, fc, H/L ratio and %PWR in various bandwidths are commonly used indices and were therefore chosen to be studied. A total bandwidth over 15-250 Hz. was considered. A low end cut-off of 15 Hz. was felt to be the lowest significant frequency that the EMG signal could be detected without including movement artifact. Previous investigators (Schweitzer et al, 1979) found little activity above 250 Hz. and so this was chosen to be the upper cut-off point. To increase this value would provide no further pertinent information and would only reduce the number of channels sampled or the sampling period.

Total PWR indicated the activity of a muscle in a similar manner to MRE and RMSE but was more sensitive to changes in force as it varied with the square of MRE and RMSE. It provided no further useful information.

Analyses of the spectral indices using three-way ANOVA's ($P<0.05$) indicated a dramatic shift to higher frequency power within the spectrum with increasing knee-joint angle. Curare on the other hand did not seem to have a significant effect although it produced a trend of increasing lower frequency power.

The apparent rise in frequency power with increasing joint angle is most likely the result of a change in the perception of the EMG signal by the surface electrodes. Schweitzer et al (1979) found a similar action during the course of inspiration using diagphramatic electromyograms. They attributed the rise in frequency power to recruitment of additional motor units, characterized by shorter action potentials. In this study however, recruitment may vary as the knee extends but is unlikely to be the sole or greatest source contributing to the shift. The almost linear increase in f_c with increasing knee-joint angle, suggests that change in muscle geometry underlying the electrodes may be the key source. One factor to consider with this geometry variation is that as the fibres shorten relative to the distance between the electrodes, the EMG may have an apparent increase in high frequency components due to an apparent increased conduction velocity. Another factor is the change in angle of the fibres with respect to the line between the electrodes as the knee extends or flexes. The spectrum may not actually change but the electrodes may "see" something different since the direction the action potentials travel may vary. Changing muscle bulk and stretching of the skin may also contribute to the observed action by allowing more signal to be perceived by the surface electrodes. Unfortunately, the spectral analysis cannot differentiate the mechanisms involved and the contributions of each can only be hypothesized.

The trend to lower frequency power with curare is more difficult to account for. A spectral shift downwards is usually thought to be a result of a decrease in conduction velocity or to a synchronization of motor units during fatigue studies (Lindstrom, 1970). However, neither of these factors seem likely in this study. As far as is presently known, curare does not have any effect along the length of the muscle fibre away from the neuromuscular junction and so could not affect conduction velocity. Also, there was no evidence of synchronization during contractions.

Assuming that curare only affects the freqency of action potentials and not their duration, the reduction of frequency power must include the addition of motor units with lower spectral power (ie. larger units). This lower power may be due to longer action potential durations or to deeper fibres being recruited. These deeper fibres have lower frequencies as a result of the low-pass filter (Lynn et al, 1978) qualities of tissue between the electrodes and the fibres. As the distance from the fibres to the electrodes increases the bandwidth of signal "seen" is reduced.

The lowering of frequency power may also derive from the fashion in which the action potentials summate across motor units as not all of an individual unit will contribute to the overall signal resulting in a shift to lower frequencies. Consequently, the monitored signal may resemble synchronization.

CHAPTER V

CONCLUSIONS

The relation between knee-joint position and maximum torque output of the quadriceps was similar to that found previously ie. torque decreases when the joint angle increases. Classical force-length characteristics of muscle, as well as mechanical leverage variation account for this action. A similar action with curare was observed but with maximum force levels reduced relative to the level of dosage and not by equal amounts at all joint angles.

Curare did not have a significant effect on the force-integrated-surface EMG relationship in the quadriceps as had been observed in past studies with the human diagphram. Although this lack of effect was unexpected, it was a more logical observation. In the curarized state it is hypothesized that more motor units are recruited to perform the same function than in the normal state, but these fire at a reduced rate. Surface electrodes cannot distinguish the integrated EMG between the two conditions.

The slope of the force-EMG relationship increased as the lower leg lifted (knee-joint angle increased). This phenomenon can be attributed to force-length characteristics of muscle, mechanical advantages around the knee, motor unit recruitment, and muscle and electrode geometry.

Power spectral analyses provided a wealth of information but the value of all the information computed is dubious. Centroid frequency provided the most stable and reproduceable index and was the best index for the comparison of one spectrum with another. However, fc did not show spectral shape variation as well as the more unstable %PWR in bands and H/L ratios.

An increase in frequency power was observed when the joint angle increased. This was most likely the result of perceptual monitoring differences by the surface electrodes to the EMG signal as the knee extended rather than actual spectral shifts, caused by action potential shape variations.

Although there were no statistically significant differences in spectra of curarized muscle when compared with normal muscle, a trend to increasing low frequency power can be attributed to the action of curare. Recruitment of motor units that are either deeper or have longer action potential durations or both is the most likely explain-ation. An unusual summation of the action potentials in this state may also contribute to the slight increase in low frequency power, and to the reduction in centroid frequency.

APPENDIX 1

DATA MANIPULATION EXAMPLES

APPENDIX 1-A

HANNING WINDOW

The input data vector is multiplied by a function resembling a cosine bell on a pedestal as follows:

$$x_t \times \frac{1}{2} \left(1 - \cos\frac{2\pi t}{T}\right) \qquad 0 < t < T-1$$

where x_t is an element in the data vector.

APPENDIX 1-B

CALCULATION OF REGRESSION COEFFICIENTS OF TORQUE-MRE RELATIONSHIPS

(1) Straight line relationship:

$$MRE = B \times T$$

$$B = \frac{\sum xy}{\sum x^2}$$

where x = Torque

y = MRE

$$r^2 = \frac{(\sum xy)^2}{\sum x^2 \sum y^2}$$ -coefficient of determination uncorrected for the mean

(2) Quadratic relationship:

$$MRE = B_1 \times T + B_2 \times T^2$$

$$\begin{bmatrix} B_1 \\ B_2 \end{bmatrix} = \frac{1}{\sum x^2 \sum x^4 - (\sum x^3)^2} \begin{bmatrix} \sum x^4 & -\sum x^3 \\ -\sum x^3 & \sum x^2 \end{bmatrix} \begin{bmatrix} \sum xy \\ \sum x^2 y \end{bmatrix}$$

where x = Torque

y = MRE

$$r^2 = \frac{B_1 \sum xy + B_2 \sum x^2 y}{\sum y^2}$$ -coefficient of determination uncorrected for the mean

EXAMPLES OF CALCULATING REGRESSION COEFFICIENTS

Subject K.K., Vastus Medialis @90°

TORQUE (x)	MRE (y)
131	102
131	91
95	68
98	63
64	57
68	50
32	32
34	34

$$y^2 = 35.2 \times 10^3$$

$$x^2 = 63.9 \times 10^3$$

$$x^3 = 6.94 \times 10^6$$

$$x^4 = 803 \times 10^6$$

$$xy = 47.1 \times 10^3$$

$$x^2y = 5.07 \times 10^6$$

$$x^3y = 585 \times 10^6$$

$$x^4y = 70.3 \times 10^9$$

Linear Relationship

$$B = \frac{47.1 \times 10^3}{63.9 \times 10^3} = 0.74$$

$$r^2 = \frac{(47.1 \times 10^3)^2}{(63.9 \times 10^3)(35.2 \times 10^3)} = 0.99$$

Quadratic Relationship

$$\begin{matrix} B_1 \\ B_2 \end{matrix} = \frac{1}{(63.9\text{x}10^3)^2(803\text{x}10^6)^2 - (6.94\text{x}10^6)^2} \begin{bmatrix} 803\text{x}10^6 & -6.94\text{x}10^6 \\ -6.94\text{x}10^6 & 63.9\text{x}10^3 \end{bmatrix} \begin{bmatrix} 47.1\text{x}10^3 \\ 5.07\text{x}10^6 \end{bmatrix}$$

$$B_1 = 0.87$$

$$B_2 = -0.001$$

$$r^2 = \frac{0.87(47.1\text{x}10^3) + (-0.001)(5.07\text{x}10^6)}{35.2\text{x}10^3}$$

$$r^2 = 0.99$$

APPENDIX 1-Ca

3-WAY ANOVA TESTING THE SIGNIFICANCE OF VARIOUS SOURCES AFFECTING LINEAR TORQUE-MRE RELATIONSHIPS @ T=25 N-m

Subjects	n	ΣMRE	$(\Sigma \text{MRE})^2$	ΣMRE^2	MRE(avg)
K.M.	6	285	81225	19704	48
K.K.	6	180	32490	6578	30
F.B.	6	229	52281	12660	38
F.S.	6	358	128092	29218	60
	24	1052	294088	68160	44(avg)

$$SS = \frac{294088}{6} - \frac{1052^2}{24} = 49015 - 46113 = 2902$$

Angles	n	ΣMRE	$(\Sigma \text{MRE})^2$	ΣMRE^2	MRE(avg)
90°	8	176	30797	4010	22
120°	8	249	62066	4741	31
150°	8	627	393355	55408	78
	24	1052	486218	68160	44(avg)

$$SS = \frac{486218}{8} - \frac{1052^2}{24} = 60777 - 46113 = 14665$$

Condition	n	ΣMRE	$(\Sigma \text{MRE})^2$	ΣMRE^2	MRE(avg)
Control	12	467	217828	25469	39
Curare	12	585	342319	42691	49
	24	1052	560147	68160	44(avg)

$$SS = \frac{560417}{12} - \frac{1052^2}{24} = 46701 - 46113 = 588$$

Source	df	SS	MS	F	F_{table} (P<0.05)
Subjects	3	2902	967	4.22*	3.20
Angles	2	14665	7333	32.0*	5.59
Condition	1	588	588	2.57	4.45
Residual	17	3892	229		
Total	24	68160			
Mean	1	46113			
Total (corrected for the mean)	23	22047			

* significant @ P<0.05

APPENDIX 1-Cb

3-WAY ANOVA TESTING THE SIGNIFICANCE OF VARIOUS SOURCES AFFECTING QUADRATIC TORQUE-MRE RELATIONSHIPS @ T=25 N-m

Subjects	n	ΣMRE	$(\Sigma MRE)^2$	ΣMRE^2	MRE(avg)
K.M.	6	303	91561	22656	50
K.K.	6	199	39661	8665	33
F.B.	6	199	39772	10477	33
F.S.	6	346	119585	32021	58
	24	1047	290579	73819	44(avg)

$$SS = \frac{290579}{6} - \frac{1047^2}{24} = 48429 - 45675 = 2754$$

Angles	n	ΣMRE	$(\Sigma MRE)^2$	ΣMRE^2	MRE(avg)
90°	8	167	27786	3548	21
120°	8	206	42407	6711	26
150°	8	674	454761	63560	84
	24	1047	524954	73819	44(avg)

$$SS = \frac{524954}{8} - \frac{1047^2}{24} = 65619 - 45675 = 19944$$

Condition	n	ΣMRE	$(\Sigma MRE)^2$	ΣMRE^2	MRE(avg)
Control	12	466	217315	30893	39
Curare	12	581	337340	42926	48
	24	1047	554655	73819	44(avg)

$$SS = \frac{554655}{12} - \frac{1047^2}{24} = 46221 - 45675 = 546$$

Source	df	SS	MS	F	F_{table} (P<0.05)
Subjects	3	2754	918	3.19	3.20
Angles	2	19944	9972	34.6*	5.59
Condition	1	546	546	1.90	4.45
Residual	17	4900	288		
Total	24	73819			
Mean	1	45675			
Total (corrected for the mean)	23	28144			

* significant @ P<0.05

APPENDIX 1-D

3-WAY ANOVA TESTING THE SIGNIFICANCE OF VARIOUS SOURCES AFFECTING CENTROID FREQUENCY

Averaged f_c values for Vastus Medialis:

Knee angle	90°		120°		150°	
Subject	Control	Curare	Control	Curare	Control	Curare
K.M.	73.3	71.8	84.8	85.1	85.1	87.9
K.K	68.6	73.5	75.3	72.3	80.1	73.0
F.B	69.0	67.6	75.6	77.9	90.8	76.0
F.S	61.8	64.8	78.3	75.1	84.8	80.3

Subjects	n	Σf_c	$(\Sigma f_c)^2$	Σf_c^2	f_c(avg)
K.M.	6	488.0	238144	39930	81.3
K.K.	6	442.8	196072	32751	73.8
F.B.	6	456.9	208758	35135	76.2
F.S.	6	445.1	198114	33428	74.2
	24	1832.8	841088	141244	76.4(avg)

$$SS = \frac{841088}{6} - \frac{1832.8^2}{24} = 140181 - 139965 = 216$$

Angles

	n	Σf_c	$(\Sigma f_c)^2$	Σf_c^2	f_c(avg)
90°	8	550.4	302940	37985	68.8
120°	8	624.4	389875	48885	78.1
150°	8	658.0	432964	54373	82.3
	24	1832.8	1125779	141244	76.4(avg)

$$SS = \frac{1125779}{8} - \frac{1832.8^2}{24} = 140722 - 139965 = 757$$

Condition

	n	Σf_c	$(\Sigma f_c)^2$	Σf_c^2	f_c(avg)
Control	12	927.5	860256	72460	77.3
Curare	12	905.3	819568	68784	75.4
	24	1832.8	1679824	141244	76.4(avg)

$$SS = \frac{1679824}{12} - \frac{1832.8^2}{24} = 139985 - 139965 = 20$$

Source	df	SS	MS	F	F_{table} (P<0.05)
Subjects	3	216	72.0	4.28*	3.20
Angles	2	757	378.5	22.5*	5.59
Condition	1	20	20.0	1.18	4.45
Residual	17	286	16.8		
Total	24	141244			
Mean	1	139965			
Total (corrected for the mean)	23	1279			

* significant @ P<0.05

APPENDIX 2

FORTRAN LISTINGS

APPENDIX 2-A

DATA PROCESSING WITH POWER SPECTRUM DISPLAY

```
 DIMENSION IDAT(2000),IOUT(1024),IX(1024),SPEC(2048)
 DIMENSION IWK(12),AXIS(4,4),DATA(2048),IFDATA(2048)
 DIMENSION ISPEC(20,3),IEL(3,2),IBFREQ(3,2)
 DIMENSION ABTOT(3,),IFILE(7),IHLB(4),IIHLB(4),ADATA(2048)
 COMPLEX DATA
C
 EQUIVALENCE (DATA,IDAT,SPEC),(IFDATA,IOUT)
 DATA NNO,IYES/'NO','YE'/
 WRITE(7,100)
100 FORMAT (TOT. NO. OF. REC. AND WORDS PER REC?'/1X,'*** ****)
 READ(5,200)NTOT,NREC
200 FORMAT(I3,1X,I4)
 DEFINE FILE 1 (NTOT,NREC,U,JREC)
 WRITE(7,101)
101 FORMAT(' WHAT IS DATA FILE NAME?'/)
 READ(5,201)(IFILE(J),J=1,7)
 CALL ASSIGN(1,IFILE,14,'RDO')
201 FORMAT(7A2)
 WRITE(7,102)
102 FORMAT(' WHAT IS THE SAMPLE RATE AND FREQ. WIDTH?'/' **** ****')
 READ(5,202)ISAMP,IFREQ
202 FORMAT(I4,1X,I4)
 WRITE(7,103)
103 FORMAT(' WHAT ARE FREQ. BANDS (HZ.)?/' ***_***')
 DO 300 I=1,3
300 READ(5,203)(IBFREQ(I,J),J=1,2)
203 FORMAT(2(I3,1X))
 WRITE(7,104)
104 FORMAT(' WHAT ARE FREQ. BANDS FOR H/L RATIO (HZ.)?'/
     +  ' LOW BAND',2X,'HIGH BAND'/' *** *** *** ***')
 READ(5,204)(IIHLB(J),J=1,4)
204 FORMAT(4(I3,1X,))
 WRITE(7,105)
105 FORMAT(' WHAT IS WINDOW POSITION IN TIME?'/' *.* *.*')
 READ(5,205)FW1,FW2
205 FORMAT(2(F3.1,1X))
C
 IW1+(ISAMP*1.)*FW1+1
 IW2=(ISAMP*1.)*FW2
 IFWIND=(IW2-IW1+1)*1.5
 IVECT=0
 DO 301 I=1,11
 IFWIND=IFWIND/2
 IF(IFWIND.EQ.0)GO TO 302
 IVECT=IVECT+1
301 CONTINUE
302 IFWIND=2**IVECT
 IHWIND=IFWIND/2
C
```

```
304 WRITE(7,106)
106 FORMAT(' WHAT IS THE REC. NO. AND AMP. MULT.?'/' *** ***)
 READ(5,206)IREC,IMULT
206 FORMAT(I3,1X,I3)
 SCAL=(17./10.05)*1023.
 DELTAF=ISAMP/(1.*IFWIND)
 INUM=((IFREQ*1.)/DELTAF)+1
 DO 306 I=1,3
 DO 305 J=1,2
305 IEL(I,J)=((IBFREQ(I,J)*1.)/DELTAF)+1
306 CONTINUE
C
 IX(1)=0
 XTEMP=0
 DO 307 I=2,INUM
 XTEMP=XTEMP+DELTAF
C MULT. BY 15 TO AVOID TRUNCATION
 IX(I)=XTEMP*15.
307 CONTINUE
 SMULT=SCAL/IX(INUM)
C HASH MARK 5HZ FOR !KHZ SAMPLE RATE
C 10 HZ FOR 2KHZ SAMPLE RATE
 IHASH=(ISAMP*15)/200
C
 AXIS(1,1)=0
 AXIS(1,2)=17.
 AXIS(1,3)=.25
 AXIS(1,4)=0
 IERAS=1
 CALL AXPLOT(AXIS,4,4,1,SMULT,1.,1.7,IHASH,IERAS)
 IERAS=0
 XO=1
 CALL SCALE(IX,1024,1,INUM,XO,SMULT)
 YO=1.7
 KK=IW1-1
 READ(1'IREC)(IDAT(J),J=1,NREC)
C
 DO 308 J=1,IFWIND
308 IFDATA(J)+IDAT(J+KK)
 DO 10 J=1,IFWIND
 ADATA(J)=FLOAT(IFDATA(J))/409.6
10 CONTINUE
 ROFF=0
 DO 20 J=1,IFWIND
 ROFF=ROFF+ADATA(J)
20 CONTINUE
 ROFF=ROFF/IFWIND
 DO 30 J=1,IFWIND
 ADATA(J)=ADATA(J)-ROFF
30 CONTINUE
```

```
      MRE=0
      RMS=0
      DO 40 J=1,IFWIND
      MRE=MRE+ABS(ADATA(J))
      RMS=RMS+ADATA(J)**2
   40 CONTINUE
      MRE=MRE/IFWIND
      RMS=SQRT(RMS/IFWIND)
      DO 309 J=1,IFWIND
      XTEMP=FLOAT(IFDATA(J))/409.6
      PI=3.141592654
      XTEMP=XTEMP*.5(1-COS(2*PI*J/1024.))
      DATA(J)=CMPLX(XTEMP,0)
  309 CONTINUE
      CALL FFT2(DATA,IVECT,IWK,2048,12)
      DO 310 J=1,IFWIND
      XTEMP=CABS(DATA(J))
      XTEMP=XTEMP*XTEMP
  310 CONTINUE
C
      CALL FUNSH(SPEC(1),IFWIND,IVECT)
      SCAL2=(6./19.05)*1023.
      SPEC(1)=0
      PTOT=0
      DO 311 J=1,IHWIND
      PTOT=PTOT+SPEC(J)
  311 CONTINUE
C
      DO 312 J=1,3
      BPTOT=0
      IST=IEL(J,1)
      IET=IEL(J,2)
      IBTOT=IET-IST+1
      DO 313 JJ=IST,IET
  313 BPTOT=BPTOT+SPEC(JJ)
      ABTOT(J)=BPTOT/PTOT*100
  312 CONTINUE
C
      DO 314 J=1,INUM
  314 IOUT(J)=IFIX((SPEC(J)/PTOT)*SCAL2*IMULT)
      CALL SCALE(IOUT,1024,1,INUM,YO,1.)
      CALL PLOTEK(IX(1),IOUT(1),INUM,1,0,0)
C
C CALCULATE MEDIAN FREQ.
      SUM=SPEC(1)
      DO 315 I=2,IHWIND
  315 SUM=SUM+SPEC(I)*DELTAF*(I-1)
      IMED=IFIX(SUM/PTOT)
C
```

```
C CALCULATE H/L RATIO
 DO 316 J=1,4
316 IHLB(J)=(IIHLB(J)*1.)/DELTAF+1
 HBPTOT=0
 BBPTOT=0
 IL1=IHLB(1)-1
 IL2=IHLB(2)-IHLB(1)+1
 IH1=IHLB(3)-1
 IH2=IHLB(4)-IHLB(3)+1
 DO 317 I=1,IL2
317 BBPTOT=BBPTOT+SPEC(IL1+1)
 DO 318 I=1,IH2
318 HBPTOT=HBPTOT+SPEC(IH1+1)
 RATIO=HBPTOT/BBPTOT
C
 CALL PLOTEK(0,780,1,1,0,0)
 CALL HOME
 WRITE(9,400)(IFILE(J),J=3,7),IREC
400 FORMAT(5X,'FILE: ',5A2,5X,'RECORD NO. ',I3)
 WRITE(9,401)FW1,FW2,IMULT
401 FORMAT(5X,'WINDOW FROM ',F3.1,' SEC TO ',F3.1,' SEC',5X,'MULT:'I3)
 WRITE(9,402)((IBFREQ(I,J),J=1,2),I=1,3)
402 FORMAT(/,5X,'FREQ. BANDS:',6X,3(I3,' - ', I3,5X))
 WRITE(9,403)(ABTOT(J),J=1,3)
403 FORMAT(5X,'%POWER IN BAND:',6X,3(F3.0,11X))
 WRITE(9,404)IFREQ,PTOT
404 FORMAT(/,5X,'TOTAL POWER IN ',I4,' HZ. BAND=',E9.3)
 WRITE(9,405)IMED
405 FORMAT(5X,'THE MEDIAN FREQ. IS ',I3,' HZ.')
 WRITE(9,406) RATIO,(IIHLB(J),J=1,4)
406 FORMAT(5X,'THE H/L RATIO IS=',F5.3,' FOR BANDS ',2(I3,'-'I3,2X))
 WRITE(9,407)MRE
407 FORMAT(5X,'THE MRE IS=',E9.3,' MV')
 WRITE(9,408)RMS
408 FORMAT(5X,'THE RMS EMG IS=,E9.3,'MV')
 REWIND 9
C
 WRITE(7,107)
107 FORMAT(' ANOTHER DISPLAY?')
 READ(5,207)IDEC
207 FORMAT(A2)
 IF(IDEC.EQ.IYES) GO TO 304
 END
```

APPENDIX 2-B

TORQUE CALCULATION

```
 DIMENSION IDATA(2000),IDATB(2000),IDATC(2000)
 DIMENSION IOUTA(2000),IOUTB(2000),IOUTC(2000)
 DIMENSION FORCE(100),IFILEA(7),IFILEB(7),IFILEC(7)
C
 WRITE(7,100)
100 FORMAT(' TOT. NO. OF REC. AND WORDS PER REC.?'/' *** ****')
 READ(5,200)NTOT,NREC
200 FORMAT(I3,,1X,I4)
 DEFINE FILE 1 (NTOT,NREC,U,JREC)
 DEFINE FILE 2 (NTOT,NREC,U,KREC)
 WRITE(7,110)
110 FORMAT(' WHAT DATA FILE CONTAINS ZERO CALIB.?')
 READ(5,210)(IFILEA(J),J=1,7)
210 FORMAT(7A2)
 CALL ASSIGN(1,IFILEA,14,'RDO')
 WRITE(7,120)
120 FORMAT(' REC. NO. WITH ZERO?'/' ***')
 READ(5,220)IRECA
220 FORMAT(I3)
 READ(1'IRECA)(IDATA(J),J=1,NREC)
 CALL AVG(IDATA,IOUTA,2000,1,2000,25)
 ZERO=0
 DO 300 J=1,NREC
 ZERO=ZERO+IDATA(J)
300 CONTINUE
 IZERO=ZERO/NREC
C
 WRITE(7,130)
130 FORMAT(' WHAT DATA FILE CONTAINS MAX. CALIB.?')
 READ(5,230)(IFILEB(J),J=1,7)
230 FORMAT(7A2)
 CALL ASSIGN(2,IFILEB,14,'RDO')
 WRITE(7,140)
140 FORMAT(' REC. NO. WITH MAX.? MAX. TORQUE?'/' *** ***.**')
 READ(5,240)IRECB,XMAX
240 FORMAT(I3,1X,F6.2)
 READ(2'IRECB)(IDATB(J),J=1,NREC)
 CALL AVG(IDATB,IOUTB,2000,1,2000,25)
 ILARGE=IDATB(1)
 DO 310 J=2,NREC
 IF(IDATB(J).GT.ILARGE)ILARGE=IDATB(J)
310 CONTINUE
 ITEMP=ILARGE-IZERO
 FACTOR=XMAX/ITEMP
C
```

```
 WRITE(7,150)
150 FORMAT(' WHAT IS DATA FILE NAME?')
 READ(5,250)(IFILEC(J),J=1,7)
250 FORMAT(7A2)
 WRITE(7,160)
160 FORMAT(' NO. OF REC.?'/' **')
 READ(5,260)MTOT
260 FORMAT(I2)
 DEFINE FILE 3 (MTOT,NREC,U,LREC)
 CALL ASSIGN(3,IFILEC,14,'RDO')
 DO 320 IRECC=1,MTOT,4
 READ(3'IRECC)(IDATC(J),J=1,NREC)
 CALL AVG(IDATC,IOUTC,1,2000,25)
 SUM=0
 DO 330 J=500,1524
330 SUM=SUM+IDATC(J)
 FORCE(IRECC)=FACTOR*((SUM/1025)-IZERO
320 CONTINUE
 CALL PLOTEK(0,780,1,1,0,1)
C
 CALL HOME
 WRITE(9,400)(IFILEC(J),J=3,7)
400 FORMAT(5x,'FILE ',5A2)
 WRITE(9,410)
410 FORMAT(5X,'REC. NO.',5X,'FORCE (N-M)')
 DO 340 I=1,MTOT,4
 WRITE(9,420)I,FORCE(I)
420 FORMAT(5X,I5,8X,F6.2/)
340 CONTINUE
 REWIND 9
 END
```

APPENDIX 3

RAW DATA

F.S.

CH 1
90

FORCE N-M	SRE μV	RMS μV	fc Hz	H/L	L-BAND % PWR	M-BAND % PWR	H-BAND % PWR	TOTAL PWR
				CONTROL				
215	93	127	78	0.482	37.5	44.4	18.1	748
218	97	132	85	0.771	25.9	54.2	19.9	748
221	111	152	82	0.588	28.5	54.7	16.8	926
148	67	91	79	0.466	30.9	54.8	14.4	482
141	62	80	81	0.630	31.0	49.5	19.5	339
98	51	67	76	0.383	29.6	59.0	11.3	216
98	72	95	79	0.564	25.6	59.9	14.4	383
47	43	58	78	0.423	26.9	61.7	11.4	154
46	64	83	83	0.756	18.7	67.2	14.1	337
				CURARE				
128	86	108	80	0.655	31.6	47.8	20.7	492
151	111	143	85	0.802	22.6	59.2	18.2	913
154	88	113	85	0.808	24.0	56.6	19.4	565
100	59	75	79	0.492	30.7	54.2	15.1	221
92	41	54	80	0.603	26.9	56.9	16.2	124
92	55	69	80	0.647	24.7	59.3	16.0	208
40	25	33	70	0.254	32.2	59.6	8.2	46
43	28	37	75	0.298	27.3	64.6	8.1	79

F.S. CH 2

90

FORCE N-M	SRE µV	RMS µV	fc Hz	H/L	L-BAND % PWR	M-BAND % PWR	H-BAND % PWR	TOTAL PWR
				CONTROL				
215	217	281	65	0.154	43.3	50.0	6.7	3390
218	234	304	67	0.222	34.4	58.0	7.6	4620
221	258	339	70	0.245	32.5	59.5	8.0	4610
148	105	136	66	0.219	44.7	45.5	9.8	913
141	101	129	71	0.308	31.8	58.5	9.8	823
98	66	88	65	0.227	48.1	41.0	10.9	347
98	83	105	70	0.263	42.5	46.3	11.2	478
47	40	51	70	0.283	49.5	36.5	14.0	111
46	45	58	79	0.491	36.3	45.8	17.8	162
				CURARE				
128	141	179	69	0.336	36.1	51.7	12.1	1500
151	151	191	68	0.302	37.0	51.8	11.2	1940
154	147	183	66	0.208	42.8	48.4	8.9	1570
100	106	135	77	0.438	36.8	47.1	16.1	801
92	58	72	70	0.301	37.3	51.5	11.2	234
92	96	121	69	0.256	41.9	47.4	10.7	673
40	27	34	69	0.225	50.7	37.9	11.4	46
43	37	47	67	0.239	44.9	44.3	10.7	119

FORCE N-M	SRE µV	RMS µV	fc Hz	H/L	L-BAND % PWR	M-BAND % PWR	H-BAND % PWR	TOTAL PWR
				CONTROL				
215	243	334	55	0.079	59.8	35.4	4.7	5910
218	223	289	59	0.120	55.9	37.3	6.7	3640
221	256	358	63	0.153	46.0	47.0	7.0	5090
148	121	159	56	0.116	60.0	33.0	7.0	1590
141	100	128	72	0.386	31.4	56.4	12.1	784
98	82	106	58	0.138	54.0	38.5	7.5	557
98	100	125	62	0.173	44.6	47.7	7.7	745
47	49	62	68	0.225	39.0	52.2	8.8	180
46	72	92	63	0.187	41.4	50.8	7.7	413
				CURARE				
128	141	179	69	0.336	36.1	51.7	12.1	1500
151	233	287	59	0.122	44.0	50.7	5.4	3900
154	190	242	63	0.171	44.0	48.4	7.5	2490
100	134	169	65	0.199	38.6	53.8	7.7	1120
92	75	96	70	0.327	35.2	53.2	11.5	373
92	119	150	69	0.236	33.5	58.6	7.9	899
40	43	57	59	0.113	50.7	43.5	5.7	128
43	45	57	64	0.202	42.5	48.9	8.6	137

F.S.
CH 1

120

FORCE N-M	SRE μV	RMS μV	fc Hz	H/L	L-BAND % PWR	M-BAND % PWR	H-BAND % PWR	TOTAL PWR
				CONTROL				
130	98	136	83	0.622	36.6	40.6	22.8	1060
136	95	131	95	1.260	21.7	51.0	27.3	794
124	91	123	110	2.472	15.5	46.3	38.3	685
122	97	129	111	2.802	14.0	46.8	39.2	816
95	55	73	112	2.372	17.9	39.6	42.5	223
97	69	90	110	2.915	13.2	48.4	38.4	374
49	24	32	94	1.252	21.6	51.5	27.0	46
48	39	52	98	1.705	17.4	52.8	29.7	124
				CURARE				
100	123	161	107	1.841	18.4	47.7	33.9	1350
75	85	110	105	2.329	17.0	43.5	39.5	594
55	62	79	98	1.503	20.3	49.3	30.4	293
32	37	48	98	1.487	21.6	46.2	32.2	109
51	62	80	92	1.103	23.2	51.2	25.6	316
45	47	60	90	0.932	26.1	49.5	24.4	177
44	48	64	101	1.851	17.9	49.0	33.1	222
46	46	60	82	0.771	27.8	50.7	21.5	162

F.S.
CH 2
120

FORCE N-M	SRE μV	RMS μV	fc Hz	H/L	L-BAND % PWR	M-BAND % PWR	H-BAND % PWR	TOTAL PWR
				CONTROL				
130	304	401	71	0.252	38.0	52.5	9.6	7920
136	281	361	75	0.400	31.4	56.1	12.5	6130
124	270	347	82	0.549	24.2	62.6	13.3	4720
122	261	340	80	0.520	25.4	61.4	13.2	5650
95	180	231	82	0.568	22.7	64.4	12.9	2240
97	172	219	82	0.612	24.0	61.3	14.7	2410
49	70	87	75	0.408	27.6	61.1	11.3	362
48	71	92	73	0.362	30.4	58.6	11.0	384
				CURARE				
100	264	336	78	0.344	27.7	62.8	9.5	6610
75	144	185	80	0.533	28.0	57.1	14.9	1350
55	125	156	72	0.329	37.3	50.5	12.3	1140
32	81	105	75	0.370	37.2	49.1	13.8	530
51	125	159	74	0.322	35.6	53.0	11.5	1140
45	101	128	77	0.422	37.5	46.6	15.8	773
44	96	122	76	0.393	31.0	56.9	12.2	751
46	111	142	68	0.274	35.0	55.5	9.6	900

F.S.
CH 3
120

FORCE N-M	SRE µV	RMS µV	fc Hz	H/L	L-BAND % PWR	M-BAND % PWR	H-BAND % PWR	TOTAL PWR
				CONTROL				
130	238	326	56	0.100	60.7	33.3	6.1	5730
136	225	306	70	0.319	43.6	42.5	13.9	4070
124	209	275	80	0.515	32.1	51.4	16.5	2950
122	187	238	83	0.584	31.3	50.5	18.3	2460
95	101	131	93	1.036	24.0	51.2	24.8	781
97	128	169	86	0.879	21.3	60.0	18.7	1350
49	48	64	76	0.357	33.2	54.9	11.9	211
48	66	88	82	0.575	30.9	51.4	17.7	340
				CURARE				
100	239	314	81	0.587	25.9	58.9	15.2	5810
75	137	175	78	0.468	32.0	53.0	15.0	1390
55	132	168	73	0.340	36.3	51.3	12.4	1290
32	78	99	72	0.405	30.5	57.2	12.3	458
51	127	161	68	0.279	36.7	53.1	10.2	1290
45	107	134	77	0.388	31.3	56.5	12.2	859
44	97	125	79	0.505	30.7	53.9	15.5	725
46	104	132	73	0.396	30.4	57.6	12.0	694

F.S.
CH 1
150

FORCE N-M	SRE μV	RMS μV	fc Hz	H/L	L-BAND % PWR	M-BAND % PWR	H-BAND % PWR	TOTAL PWR
				CONTROL				
63	83	118	117	4.073	11.8	40.1	48.1	526
63	98	132	105	1.582	23.4	39.5	37.1	924
48	78	103	118	4.299	10.7	43.3	46.0	505
46	82	107	111	2.375	17.2	41.8	40.9	557
				CURARE				
36	133	168	117	3.009	15.1	39.5	45.4	1300
34	113	114	118	3.188	14.0	41.2	44.8	978
16	53	69	107	2.435	16.1	44.8	39.1	244
19	56	72	101	1.311	24.7	43.0	32.4	229

F.S.
CH 2
150

FORCE N-M	SRE μV	RMS μV	fc Hz	H/L	L-BAND % PWR	M-BAND % PWR	H-BAND % PWR	TOTAL PWR
				CONTROL				
63	235	304	82	0.725	23.0	60.3	16.7	3440
66	272	351	75	0.370	32.5	55.5	12.0	7070
48	224	286	86	0.783	25.2	55.1	19.7	4280
46	208	271	88	0.834	26.0	52.4	21.7	3540
				CURARE				
36	230	295	74	0.361	28.7	61.0	10.3	4650
34	172	219	76	0.385	30.9	57.2	11.9	2420
16	127	164	83	0,637	26.9	56.0	17.1	1320
19	117	148	77	0.346	38.1	48.8	13.2	1040

F.S.
CH 3
150

FORCE N-M	SRE µV	RMS µV	fc Hz	H/L	L-BAND % PWR	M-BAND % PWR	H-BAND % PWR	TOTAL PWR
				CONTROL				
63	160	218	88	0.878	27.8	47.8	24.4	1660
66	195	259	75	0.398	40.2	43.7	16.0	3780
48	149	192	93	0.932	27.8	46.3	25.9	1760
46	154	198	83	0.606	33.3	46.6	20.2	1760
				CURARE				
36	205	263	79	0.506	36.1	45.7	18.3	3280
34	155	194	87	0.873	25.7	51.8	22.5	1820
16	109	139	79	0.439	34.2	50.8	15.0	1030
19	98	126	76	0.386	40.1	44.4	15.5	769

CH 1
90

FORCE N-M	SRE μV	RMS μV	fc Hz	H/L	L-BAND % PWR	M-BAND % PWR	H-BAND % PWR	TOTAL PWR
				CONTROL				
131	102	133	66	0.295	47.4	38.7	14.0	861
131	91	117	68	0.288	41.6	46.3	12.0	727
95	68	88	66	0.242	44.0	45.4	10.7	402
98	63	84	68	0.235	41.3	49.0	9.7	366
64	57	74	66	0.253	33.7	57.8	8.5	279
68	50	65	75	0.401	26.3	63.1	10.6	187
32	32	41	72	0.319	32.5	57.2	10.4	77
34	34	43	68	0.267	29.2	63.0	7.8	91
				CURARE				
62	60	76	75	0.359	34.5	53.1	12.4	262
78	69	88	75	0.448	29.7	56.9	13.3	326
82	73	95	70	0.309	45.2	40.8	14.0	393
72	71	92	76	0.372	32.3	55.7	12.0	345
62	54	68	72	0.380	35.8	50.6	13.6	246
62	58	75	75	0.433	30.7	56.1	13.3	221
30	30	38	75	0.605	24.4	60.8	14.8	70
32	38	49	70	0.285	30.8	60.4	8.8	131

K.K.
CH 2
90

FORCE N-M	SRE µV	RMS µV	fc Hz	H/L	L-BAND % PWR	M-BAND % PWR	H-BAND % PWR	TOTAL PWR
				CONTROL				
131	143	194	82	0.589	32.4	48.6	19.1	1800
131	122	174	80	0.456	37.5	45.4	17.1	1360
95	79	108	84	0.666	31.5	47.6	21.0	596
98	87	114	78	0.534	31.2	52.2	16.6	624
64	62	84	75	0.396	40.5	43.4	16.0	338
68	57	75	78	0.432	35.2	49.6	15.2	245
32	45	62	67	0.260	43.5	45.1	11.3	197
34	40	53	71	0.340	38.5	48.5	13.1	123
				CURARE				
62	84	116	73	0.320	43.1	43.2	13.8	540
78	101	132	65	0.242	44.9	44.3	10.9	703
82	96	121	69	0.276	42.8	45.4	11.8	705
72	81	103	69	0.311	41.2	46.0	12.8	493
62	64	83	68	0.272	40.1	49.0	10.9	323
62	75	97	76	0.456	34.9	49.2	15.9	369
30	36	46	64	0.211	50.8	38.5	10.7	96
32	37	49	71	0.339	45.0	39.7	15.3	104

K.K. CH 3
90

FORCE N-M	SRE μV	RMS μV	fc Hz	H/L	L-BAND % PWR	M-BAND % PWR	H-BAND % PWR	TOTAL PWR
				CONTROL				
131	154	209	75	0.321	29.3	61.3	9.4	2020
131	126	174	78	0.380	28.9	60.2	11.0	1560
95	76	99	74	0.271	32.4	58.8	8.8	408
98	68	88	77	0.380	35.7	50.7	13.6	355
64	39	52	63	0.146	49.9	42.9	7.3	129
68	43	56	73	0.272	35.2	55.2	9.6	153
32	19	27	60	0.142	54.0	38.3	7.7	31
34	27	35	69	0.260	42.0	47.1	10.9	56
				CURARE				
62	46	60	63	0.143	48.3	44.7	7.0	166
78	67	87	70	0.199	36.1	56.7	7.2	373
82	66	85	62	0.134	40.1	54.5	5.4	363
72	44	58	59	0.118	46.6	47.9	5.5	140
62	35	44	66	0.187	41.9	50.3	7.8	87
62	35	45	70	0.256	32.3	59.5	8.3	94
30	16	20	58	0.108	60.7	32.8	6.5	20
32	20	26	74	0.374	34.7	52.3	13.0	31

K.K. CH 1
120

FORCE N-M	SRE μV	RMS μV	fc Hz	H/L	L-BAND % PWR	M-BAND % PWR	H-BAND % PWR	TOTAL PWR
				CONTROL				
108	159	206	76	0.492	32.4	51.7	15.9	2020
98	106	140	79	0.582	32.3	48.8	18.8	923
84	139	180	82	0.581	34.2	45.9	19.9	1430
82	95	130	78	0.510	32.8	50.4	16.8	657
54	66	86	77	0.610	27.3	56.0	16.6	296
55	67	89	73	0.369	40.7	44.2	15.0	425
25	35	45	71	0.311	36.0	52.8	11.2	96
28	38	50	66	0.300	35.5	53.8	10.7	113
				CURARE				
62	77	101	74	0.397	29.4	58.9	11.7	490
53	63	81	71	0.349	38.2	48.5	13.3	271
81	81	107	68	0.311	40.0	47.6	12.4	709
79	83	108	71	0.347	38.2	48.5	13.3	555
54	55	72	75	0.422	40.1	43.0	16.9	222
53	52	66	74	0.405	31.7	55.4	12.9	189
28	33	41	75	0.637	25.5	58.3	16.2	76
25	31	40	70	0.338	31.9	57.4	10.8	72

K.K.
CH 2
120

FORCE N-M	SRE µV	RMS µV	fc Hz	H/L	L-BAND % PWR	M-BAND % PWR	H-BAND % PWR	TOTAL PWR
				CONTROL				
108	178	246	89	0.684	31.3	47.2	21.4	2870
98	124	175	87	0.906	23.3	55.6	21.1	1430
84	160	212	98	1.082	24.6	48.8	26.6	1880
82	111	149	91	0.937	25.4	50.7	23.8	934
54	71	98	90	0.781	30.5	45.7	23.8	394
55	71	99	88	0.821	28.5	48.0	23.4	496
25	40	56	82	0.613	31.3	49.6	19.2	142
28	45	61	79	0.571	27.1	57.4	15.5	190
				CURARE				
62	104	134	80	0.535	33.9	48.0	18.1	783
53	75	96	76	0.432	34.2	51.1	14.8	366
81	105	137	81	0.553	34.7	46.2	19.1	982
79	107	137	79	0.468	37.0	45.7	17.3	923
54	63	85	93	0.960	29.6	42.0	28.4	309
53	53	69	85	0.759	25.5	55.1	19.4	193
28	34	45	82	0.608	31.0	50.2	18.8	79
25	32	42	72	0.363	39.6	46.0	14.4	85

K.K.
CH 3
120

FORCE N-M	SRE µV	RMS µV	fc Hz	H/L	L-BAND % PWR	M-BAND % PWR	H-BAND % PWR	TOTAL PWR
				CONTROL				
108	245	336	100	1.497	20.2	49.5	30.3	5340
98	226	303	106	3.137	11.7	51.6	36.7	4490
84	225	313	106	2.991	11.5	54.2	34.3	3790
82	160	211	111	2.851	14.5	44.2	41.3	1940
54	77	102	95	1.368	15.3	63.8	20.9	485
55	89	118	101	2.233	12.4	59.8	27.8	563
25	44	58	97	1.324	20.7	51.8	27.4	150
28	35	46	87	0.673	24.4	59.2	16.4	83
				CURARE				
62	79	103	88	0.940	19.7	61.7	18.5	472
53	48	62	74	0.369	26.1	64.3	9.6	150
81	68	87	70	0.265	33.4	57.7	8.9	361
79	72	91	78	0.482	27.5	59.2	13.3	381
54	39	51	74	0.331	34.8	53.7	11.5	128
53	34	44	81	0.568	21.7	65.9	12.4	92
28	17	22	72	0.300	40.1	47.9	12.0	23
25	20	26	80	0.433	28.8	58.7	12.5	32

K.K.
CH 1
150

FORCE N-M	SRE μV	RMS μV	fc Hz	H/L	L-BAND % PWR	M-BAND % PWR	H-BAND % PWR	TOTAL PWR
				CONTROL				
49	191	254	78	0.423	33.7	52.1	14.3	2540
46	157	204	82	0.497	30.4	54.5	15.1	1900
36	180	232	83	0.491	32.2	52.0	15.8	2150
35	145	188	81	0.525	26.1	60.3	13.7	1390
27	114	152	78	0.464	34.4	49.6	16.0	1140
24	92	119	77	0.428	30.2	56.9	12.9	713
11	74	95	82	0.542	31.7	51.1	17.2	439
12	75	97	80	0.644	24.3	60.1	15.6	451
				CURARE				
19	87	111	74	0.356	36.1	51.0	12.9	588
21	72	95	74	0.364	35.8	51.2	13.0	380
26	70	90	68	0.267	39.1	50.4	10.5	411
27	83	106	75	0.375	30.9	57.5	11.6	537
23	67	87	71	0.294	38.0	50.8	11.2	262
25	74	95	75	0.350	38.6	47.9	13.5	417
11	48	63	74	0.389	30.8	57.3	12.0	203
11	50	65	73	0.376	29.0	60.1	10.9	201

K.K.
CH 2
150

FORCE N-M	SRE μV	RMS μV	fc Hz	H/L	L-BAND % PWR	M-BAND % PWR	H-BAND % PWR	TOTAL PWR
				CONTROL				
49	201	270	96	0.993	26.5	47.3	26.3	3020
46	174	229	105	1.581	20.7	46.6	32.7	2670
36	195	258	103	1.546	20.3	48.4	31.3	3240
35	152	203	107	1.715	19.0	48.4	32.6	1660
27	131	178	100	1.155	26.7	42.5	30.8	1490
24	98	129	108	2.004	17.1	48.7	34.2	775
11	82	108	106	1.491	21.2	47.1	31.7	557
12	71	94	113	2.396	15.7	46.8	37.5	465
				CURARE				
19	88	114	96	1.064	26.4	45.5	28.1	622
21	72	93	81	0.568	30.3	52.4	17.2	420
26	68	89	84	0.639	29.9	51.0	19.1	405
27	84	109	91	0.921	23.4	55.0	21.6	667
23	59	80	90	0.718	31.1	46.6	22.3	259
25	77	103	112	2.043	18.4	44.0	37.6	516
11	38	50	100	1.239	23.9	46.5	29.6	122
11	44	57	99	1.248	22.8	48.7	28.5	153

K.K.
CH 3
150

FORCE N-M	SRE µV	RMS µV	fc Hz	H/L	L-BAND % PWR	M-BAND % PWR	H-BAND % PWR	TOTAL PWR
				CONTROL				
49	200	265	105	2.089	16.8	48.1	35.1	3060
46	178	243	106	2.094	16.9	47.9	35.3	3440
36	165	217	104	1.852	18.3	47.7	34.0	2180
35	158	209	112	2.514	16.0	43.8	40.2	1690
27	93	122	99	1.235	23.5	47.4	29.1	739
24	83	109	108	2.433	14.8	49.1	36.0	576
11	55	72	97	1.315	21.4	50.4	28.2	218
12	68	88	112	2.373	16.7	43.8	39.6	369
				CURARE				
19	57	64	80	0.578	29.3	53.8	16.9	231
21	49	65	74	0.489	25.9	61.5	12.6	195
26	45	59	74	0.375	30.8	57.6	11.6	156
27	56	72	71	0.318	33.7	55.6	10.7	258
23	42	54	72	0.274	35.2	55.1	9.7	108
25	49	63	82	0.598	27.9	55.4	16.7	206
11	24	31	82	0.545	32.4	49.9	17.7	43
11	25	32	82	0.629	26.5	56.9	16.7	50

K.M.
CH 1
90

FORCE N-M	SRE µV	RMS µV	fc Hz	H/L	L-BAND % PWR	M-BAND % PWR	H-BAND % PWR	TOTAL PWR
				CONTROL				
199	139	184	66	0.216	46.2	43.9	10.0	1650
166	137	176	75	0.437	30.4	56.3	13.3	1390
124	81	104	74	0.474	31.9	53.0	15.1	489
129	103	133	77	0.505	36.1	45.7	18.2	650
87	65	82	76	0.525	28.4	56.6	14.9	313
90	73	94	79	0.579	32.3	49.0	18.7	396
43	31	39	75	0.539	24.6	62.2	13.2	76
50	38	49	64	0.184	44.2	49.9	5.8	86
				CURARE				
153	114	142	68	0.259	40.4	49.1	10.5	981
138	115	150	68	0.285	37.5	51.8	10.7	1070
106	61	79	73	0.432	34.5	50.6	14.9	273
111	88	115	76	0.512	25.6	61.3	13.1	589
76	43	55	72	0.423	34.9	50.4	14.8	132
81	68	89	69	0.373	37.0	49.2	13.8	373
43	55	70	74	0.401	34.8	51.2	14.0	263
46	55	71	74	0.444	30.6	55.8	13.6	251

K.M.

K.M.
CH 2
90

FORCE N-M	SRE μV	RMS μV	fc Hz	H/L	L-BAND % PWR	M-BAND % PWR	H-BAND % PWR	TOTAL PWR
				CONTROL				
199	166	219	66	0.241	40.0	50.4	9.6	2280
166	147	188	70	0.316	38.9	48.8	12.3	1650
124	95	124	67	0.265	43.1	45.5	11.4	738
129	108	141	70	0.355	39.1	47.1	13.9	859
87	64	82	65	0.205	43.9	47.1	9.0	302
90	67	89	67	0.265	33.8	57.3	8.9	358
43	30	40	61	0.132	44.2	49.9	5.8	86
50	36	49	64	0.184	46.5	44.9	8.6	99
				CURARE				
153	139	177	65	0.208	44.1	46.8	9.2	1380
138	127	166	68	0.269	43.3	45.1	11.6	1100
106	77	99	69	0.285	38.5	50.5	11.0	411
111	96	125	72	0.308	36.4	52.4	11.2	796
76	52	67	61	0.041	51.1	41.7	7.2	207
81	70	94	69	0.348	34.1	54.1	11.8	376
43	41	54	62	0.180	48.9	42.3	8.8	121
46	37	47	65	0.209	48.9	40.9	10.2	97

K.M.
CH 3
90

FORCE N-M	SRE μV	RMS μV	fc Hz	H/L	L-BAND % PWR	M-BAND % PWR	H-BAND % PWR	TOTAL PWR
				CONTROL				
199	162	207	71	0.232	30.8	62.1	7.1	2030
166	115	145	75	0.388	31.6	56.1	12.3	899
124	81	104	74	0.403	26.0	63.6	10.5	500
129	101	127	72	0.366	29.0	60.4	10.6	771
87	50	65	66	0.222	46.1	43.7	10.2	213
90	44	56	75	0.511	25.8	61.0	13.2	150
43	27	35	66	0.221	46.0	43.8	10.2	56
50	23	29	70	0.299	42.7	44.5	12.8	38
				CURARE				
153	112	143	70	0.240	35.8	55.6	8.6	985
138	81	102	69	0.295	38.8	49.7	11.5	494
106	50	65	70	0.322	36.5	51.7	11.8	160
111	47	60	73	0.320	37.2	50.9	11.9	182
76	32	40	74	0.398	36.3	49.3	14.4	76
81	33	42	68	0.336	34.2	54.3	11.5	90
43	11	14	62	0.174	55.2	35.3	9.6	10
46	12	16	69	0.371	33.7	53.8	12.5	12

K.M.
CH 1
120

FORCE N-M	SRE μV	RMS μV	fc Hz	H/L	L-BAND % PWR	M-BAND % PWR	H-BAND % PWR	TOTAL PWR
				CONTROL				
135	120	155	77	0.516	30.3	54.0	15.7	1360
117	121	159	84	0.724	27.1	53.3	19.6	1030
89	75	99	88	0.848	26.5	51.0	22.5	486
91	77	98	85	0.856	22.5	58.2	19.3	429
56	31	40	83	0.918	20.2	61.2	18.6	75
62	38	49	88	0.673	26.8	55.2	18.0	111
27	23	29	87	1.293	17.4	60.1	22.5	41
31	25	32	86	1.247	16.3	63.3	20.3	48
				CURARE				
110	75	98	87	0.919	23.4	55.0	21.5	517
111	102	135	83	0.675	29.9	50.0	20.1	967
80	77	102	93	1.107	23.3	50.9	25.8	559
79	97	127	92	0.988	23.1	54.0	22.9	802
60	41	53	87	1.106	23.1	53.4	23.5	143
51	41	53	75	0.507	30.6	53.8	15.5	138
28	26	31	81	1.032	17.7	64.1	18.3	47
29	27	33	83	1.367	15.4	63.6	21.1	52

K.M.
CH 2
120

FORCE N-M	SRE μV	RMS μV	fc Hz	H/L	L-BAND % PWR	M-BAND % PWR	H-BAND % PWR	TOTAL PWR
				CONTROL				
135	147	193	80	0.529	34.6	47.1	18.3	1990
117	148	190	81	0.601	27.2	56.5	16.3	1620
89	94	122	81	0.551	31.5	51.1	17.4	792
91	90	115	84	0.797	22.6	59.5	18.0	626
56	42	56	77	0.463	37.2	45.6	17.2	146
62	44	58	75	0.368	36.0	50.7	13.3	166
27	23	31	65	0.228	48.8	40.1	11.1	49
31	22	31	75	0.475	31.0	54.3	14.7	48
				CURARE				
110	100	133	77	0.449	37.9	45.0	17.0	927
111	149	197	76	0.430	36.0	48.5	15.5	1670
80	100	134	85	0.643	31.9	47.5	20.5	959
79	115	148	81	0.518	35.3	46.4	18.3	1100
60	51	65	84	0.617	30.4	50.8	18.8	205
51	45	58	80	0.538	31.7	51.3	17.0	151
28	20	27	74	0.430	32.3	53.8	13.9	39
29	27	36	77	0.483	32.9	51.1	15.9	67

K.M.
CH 3
120

FORCE N-M	SRE µV	RMS µV	fc Hz	H/L	L-BAND % PWR	M-BAND % PWR	H-BAND % PWR	TOTAL PWR
				CONTROL				
135	182	231	81	0.655	23.0	62.0	15.1	2520
117	136	177	89	1.136	17.4	62.9	19.7	1640
89	86	110	85	0.660	27.3	54.7	18.0	640
91	87	112	90	1.036	20.7	57.9	21.4	644
56	47	60	94	1.140	22.6	51.5	25.8	199
62	50	65	92	1.057	20.1	58.6	21.3	217
27	28	36	91	1.079	18.9	60.7	20.4	59
31	31	40	90	1.002	21.2	57.6	21.2	89
				CURARE				
110	94	122	81	0.567	24.4	61.7	13.8	709
111	92	117	75	0.400	29.0	59.4	11.6	656
80	58	74	84	0.621	27.8	54.9	17.3	274
79	54	70	77	0.554	26.7	58.5	14.8	239
60	26	34	85	0.686	30.8	48.1	21.1	50
51	26	33	80	0.639	24.4	60.1	15.6	49
28	18	23	83	0.632	27.0	55.9	17.1	25
29	15	20	73	0.389	30.6	57.5	11.9	23

K.M.
CH 1
150

FORCE N-M	SRE µV	RMS µV	fc Hz	H/L	L-BAND % PWR	M-BAND % PWR	H-BAND % PWR	TOTAL PWR
				CONTROL				
57	87	118	85	0.673	24.5	59.0	16.5	623
37	74	97	84	0.779	23.6	58.0	18.4	369
39	67	85	83	0.622	30.5	50.5	19.0	352
26	46	60	85	0.903	21.2	59.7	19.1	177
26	59	77	91	1.032	21.4	56.5	22.1	262
13	30	38	83	0.936	22.1	57.1	20.7	70
14	42	53	86	1.025	18.6	62.2	19.1	145
				CURARE				
57	108	140	92	1.086	19.4	59.5	21.1	831
51	100	133	87	0.728	25.0	56.7	18.2	950
34	77	100	93	1.072	21.1	56.3	22.6	520
32	104	140	87	0.675	25.3	57.6	17.1	1320
25	44	56	87	1.140	17.2	63.2	19.6	141
26	66	85	88	0.934	23.2	55.1	21.7	296
10	27	34	85	1.392	14.8	64.7	20.6	54
10	28	36	84	0.964	22.5	55.9	21.7	66

K.M.
CH 2
150

FORCE N-M	SRE µV	RMS µV	fc Hz	H/L	L-BAND % PWR	M-BAND % PWR	H-BAND % PWR	TOTAL PWR
				CONTROL				
57	110	148	96	1.268	19.1	56.7	24.2	909
37	95	126	86	0.690	31.9	46.1	22.0	711
39	88	116	94	1.060	25.4	47.6	26.9	613
26	65	87	88	0.782	28.5	49.3	22.2	377
26	81	109	92	0.920	28.1	46.0	25.9	546
13	41	54	88	0.792	29.2	47.8	23.1	136
14	51	69	89	0.816	30.7	44.2	25.1	235
				CURARE				
57	131	173	88	0.781	28.0	50.1	21.9	1340
51	124	165	93	0.925	25.0	51.8	23.2	1510
34	87	112	99	1.145	24.0	48.5	27.5	611
32	126	168	88	0.846	25.5	53.0	21.5	1580
25	58	76	90	0.787	28.0	50.0	22.0	311
26	80	104	89	0.851	24.1	55.2	20.7	501
10	26	36	93	1.212	20.2	55.3	24.5	64
10	34	46	97	1.091	28.3	40.8	30.9	104

K.M. CH 3
150

FORCE N-M	SRE µV	RMS µV	fc Hz	H/L	L-BAND % PWR	M-BAND % PWR	H-BAND % PWR	TOTAL PWR
				CONTROL				
57	134	170	101	1.737	18,4	49.6	32.0	1450
37	116	151	99	1.464	21.3	47.5	31.2	880
39	110	144	104	1.812	16.2	54.6	29.3	1140
26	66	84	104	1.906	15.2	55.9	28.9	296
26	75	99	111	3.066	11.6	52.7	35.7	549
13	50	67	108	1.886	18.6	46.7	34.9	205
14	51	65	102	1.515	20.6	47.5	31.6	195
				CURARE				
57	107	139	92	0.996	22.3	55.5	22.2	793
51	91	119	95	1.462	16.3	59.8	23.9	692
34	58	74	88	0.827	23.9	56.3	19.8	269
32	59	76	82	0.692	25.0	57.7	17.3	320
25	39	50	99	1.580	16.3	58.0	25.7	120
26	53	68	92	1.188	18.0	60.7	21.3	239
10	23	29	98	1.388	19.9	52.5	27.6	34
10	24	31	94	1.112	22.0	53.6	24.5	48

F.B.
CH 1
90

FORCE N-M	SRE µV	RMS µV	fc Hz	H/L	L-BAND % PWR	M-BAND % PWR	H-BAND % PWR	TOTAL PWR
				CONTROL				
211	150	186	68	0.201	31.5	62.2	6.3	1680
205	134	171	70	0.291	38.7	50.1	11.3	1290
151	105	134	72	0.247	28.0	65.1	6.9	837
99	62	80	75	0.340	29.8	60.0	10.2	243
98	64	81	71	0.316	37.1	51.2	11.7	302
48	28	36	64	0.172	43.8	48.7	7.5	68
48	34	45	63	0.144	40.2	54.0	5.8	95
				CURARE				
72	55	69	74	0.384	25.3	65.1	9.7	222
97	79	99	68	0.186	36.7	56.5	6.8	500
73	74	93	72	0.242	27.8	65.5	6.7	436
65	82	104	60	0.075	48.1	48.3	3.6	570
45	34	43	61	0.119	51.1	42.8	6.1	107
45	33	43	71	0.314	29.8	60.8	9.4	74
45	33	43	71	0.230	39.7	51.2	9.1	81
48	33	43	64	0.168	40.5	52.6	6.8	88

F.B.
CH 2
90

FORCE N-M	SRE µV	RMS µV	fc Hz	H/L	L-BAND % PWR	M-BAND % PWR	H-BAND % PWR	TOTAL PWR
				CONTROL				
211	330	422	66	0.152	36.1	58.4	5.5	9320
205	318	400	69	0.232	36.8	54.7	8.5	6410
151	378	469	65	0.141	27.6	68.5	3.9	10300
99	184	245	65	0.169	26.9	68.6	4.5	2690
98	193	243	68	0.198	32.6	61.0	6.4	2670
48	58	76	66	0.214	29.9	63.7	6.4	269
48	59	76	66	0.196	36.5	56.3	7.1	284
				CURARE				
72	96	120	69	0.192	31.2	62.8	6.0	681
97	118	148	72	0.302	28.7	62.7	8.7	995
73	98	122	65	0.155	41.3	52.3	6.4	690
65	96	123	64	0.153	34.6	60.1	5.3	647
45	46	59	70	0.241	32.9	59.2	7.9	199
45	45	57	69	0.271	32.8	58.3	8.9	122
45	38	48	66	0.225	36.8	54.9	8.3	122
48	45	59	66	0.215	38.5	53.3	8.3	160

F.B.

F.B.
CH 3
90

FORCE N-M	SRE µV	RMS µV	fc Hz	H/L	L-BAND % PWR	M-BAND % PWR	H-BAND % PWR	TOTAL PWR
				CONTROL				
211	269	338	69	0.312	26.8	64.8	8.4	5880
205	229	289	75	0.412	30.3	57.1	12.5	3540
151	202	261	68	0.314	26.8	64.8	8.4	0.309
99	105	138	74	0.481	25.7	62.0	12.3	854
98	109	142	75	0.396	28.9	59.7	11.4	891
48	54	71	69	0.299	35.9	53.3	10.8	264
48	59	77	75	0.455	26.2	61.8	11.9	318
				CURARE				
72	89	113	73	0.418	23.0	67.4	9.6	620
97	131	162	70	0.282	39.0	50.0	11.0	1360
73	115	145	70	0.261	29.3	63.0	7.7	1150
65	137	171	60	0.090	48.5	47.1	4.4	1550
45	62	80	71	0.305	40.4	47.2	12.3	328
45	61	79	76	0.420	31.1	55.8	13.1	257
45	63	82	74	0.391	27.4	61.9	10.7	328
48	62	81	76	0.454	26.2	61.9	11.9	302

F.B.
CH 1
120

FORCE N-M	SRE µV	RMS µV	fc Hz	H/L	L-BAND % PWR	M-BAND % PWR	H-BAND % PWR	TOTAL PWR
				CONTROL				
154	161	202	70	0.331	31.0	58.7	10.2	2050
154	151	192	75	0.396	33.9	52.7	13.4	1550
150	153	192	79	0.744	20.6	64.1	15.3	1630
147	149	189	77	0.520	31.9	51.5	16.6	1720
99	75	96	81	0.548	31.4	51.4	17.2	397
97	89	115	81	0.650	29.6	51.1	19.2	686
48	27	34	72	0.311	35.8	53.0	11.1	56
48	28	36	70	0.292	32.3	57.6	9.6	77
				CURARE				
41	40	51	80	0.551	25.2	60.9	13.9	132
63	62	79	82	0.653	28.6	52.8	18.7	259
62	78	99	83	0.683	30.4	48.8	20.8	446
69	81	103	78	0.616	27.1	56.2	16.7	522
44	46	60	77	0.483	38.5	42.9	18.6	170
45	32	41	79	0.539	25.5	60.7	13.7	68
45	39	49	75	0.449	32.8	52.4	14.7	131
47	38	50	69	0.302	30.1	60.8	9.1	126

F.B.
CH 2
120

FORCE N-M	SRE μV	RMS μV	fc Hz	H/L	L-BAND % PWR	M-BAND % PWR	H-BAND % PWR	TOTAL PWR
				CONTROL				
154	492	638	70	0.280	25.0	68.0	7.0	20300
154	441	565	76	0.246	35.9	55.2	8.8	15600
150	560	720	76	0.579	19.1	69.9	11.0	22100
147	597	767	79	0.804	16.5	70.3	13.2	29100
99	303	388	80	0.607	23.5	62.3	14.2	6730
97	329	419	82	0.639	24.0	60.6	15.4	7320
48	71	91	81	0.639	23.8	60.9	15.2	347
48	100	130	83	0.859	16.9	68.5	14.5	749
				CURARE				
41	71	90	70	0.200	38.1	54.3	7.6	440
63	95	121	72	0.297	33.8	56.2	10.0	635
62	116	149	68	0.209	36.6	55.8	7.6	1000
69	123	157	73	0.360	30.4	58.7	10.9	1190
44	84	108	69	0.243	36.1	55.1	8.8	635
45	52	68	65	0.211	38.5	53.4	8.1	195
45	63	81	69	0.209	40.3	51.3	8.4	318
47	60	76	70	0.280	29.0	62.8	8.1	281

F.B.
CH 3
120

FORCE N-M	SRE μV	RMS μV	fc Hz	H/L	L-BAND % PWR	M-BAND % PWR	H-BAND % PWR	TOTAL PWR
				CONTROL				
154	199	253	79	0.658	21.1	65.0	13.9	3290
154	173	222	86	0.722	23.5	59.5	17.0	2200
150	196	249	85	1.031	17.1	65.2	17.7	2790
147	187	240	83	0.744	21.5	62.5	16.0	2710
99	104	132	86	0.744	24.8	56.7	18.5	804
97	114	145	88	0.873	19.8	62.9	17.3	1130
48	40	53	97	1.252	20.1	54.7	25.2	126
48	39	53	85	0.857	23.1	57.1	19.8	143
				CURARE				
41	45	58	87	0.895	21.2	59.8	19.0	170
63	72	90	95	1.521	15.8	60.2	24.0	335
62	96	123	91	1.204	17.9	60.7	21.5	693
69	99	129	93	1.474	15.0	62.8	22.2	837
44	63	82	90	1.000	22.0	56.1	22.0	359
45	41	54	94	1.157	19.8	57.4	22.9	129
45	49	64	89	1.001	22.4	55.1	22.5	199
47	44	58	91	1.129	18.5	60.7	20.8	159

F.B.
CH 1
150

FORCE N-M	SRE μV	RMS μV	fc Hz	H/L	L-BAND % PWR	M-BAND % PWR	H-BAND % PWR	TOTAL PWR
				CONTROL				
76	153	195	86	0.877	26.0	51.1	22.8	1910
74	143	181	91	1.136	20.3	56.6	23.1	1570
49	109	138	89	0.861	27.2	49.4	23.4	861
48	84	109	97	1.325	24.3	43.5	32.2	696
				CURARE				
22	70	91	78	0.546	36.3	43.9	19.8	341
16	66	86	72	0.335	32.8	56.2	11.0	318
22	85	110	74	0.351	38.6	47.8	13.6	573
23	82	104	80	0.542	31.8	51.0	17.2	595

F.B.
CH 2
150

FORCE N-M	SRE μV	RMS μV	fc Hz	H/L	L-BAND % PWR	M-BAND % PWR	H-BAND % PWR	TOTAL PWR
				CONTROL				
76	509	658	80	0.723	17.7	69.5	12.8	22300
74	512	658	82	0.740	16.7	70.9	12.4	21000
49	438	559	84	0.645	24.1	60.4	15.5	14500
48	335	444	81	0.860	20.8	61.2	17.9	9840
				CURARE				
22	88	111	70	0.307	29.9	61.0	9.2	549
16	74	93	71	0.268	31.9	59.6	8.5	419
22	100	125	71	0.281	37.9	51.4	10.7	726
23	108	138	76	0.382	33.4	53.8	12.8	993

F.B.
CH 3
150

FORCE N-M	SRE μV	RMS μV	fc Hz	H/L	L-BAND % PWR	M-BAND % PWR	H-BAND % PWR	TOTAL PWR
				CONTROL				
76	160	205	90	1.093	17.1	64.2	18.7	21900
74	158	200	99	2.028	13.9	57.9	28.2	20000
49	132	170	92	1.179	18.8	59.1	22.1	12500
48	102	139	98	1.527	15.1	61.8	23.1	1180
				CURARE				
22	57	74	93	1.574	13.4	65.5	21.1	245
16	47	60	94	1.736	12.4	66.0	21.6	156
22	75	95	94	1.739	11.2	69.3	19.5	439
23	77	99	99	1.741	14.6	59.9	25.4	527

REFERENCES

REFERENCES

1. Albuquerque, E.X. et al. An electrophysical and morphological study of the neuromuscular junction in patients with myasthenia gravis. Exp. Neurol. 51: 536-563, 1976.

2. Alderson, A.M., and J. Maclagan. The action of decamethonium and tubocurarine on the respiratory and limb muscles of the cat. J. Physiol. 173: 38-56, 1964.

3. Bergland, G.D. A guided tour of the Fast Fourier Transform. IEEE Spectrum 6: 41-51, July 1969.

4. Bigland, B., and O.C.J. Lippold. Motor unit activity in the voluntary contraction of human muscle. J. Physiol. 125: 322-335, 1954.

5. Blackman, R.B., and J.W. Tukey. The measurement of Power Spectra. New York: Dover, 1958.

6. Brigham, E.O. The Fast Fourier Transform. Englewood Cliffs, N.J.: Prentice-Hall, 1974.

7. Bruce, E.N., M.D. Goldman, and J. Mead. A digital computer technique for analyzing respiratory muscle EMG's. J. Appl. Physiol.:Resp. Env. Exer. Physiol. 43(3): 551-556, 1977.

8. Chaffin, D.B.. Surface electromyography frequency analysis as a diagnostic tool. J. Occ. Med. 11(3): 109-115, 1969.

9. Clamann, H.P., and K.T. Broeker. Relation between force and fatiguability of red and pale skeletal muscles in man. Am. J. Phys. Med. 58(2): 70-85, 1979.

10. Clarke, H.H. et al. Relationship between body position and the application of muscle power to movements of the joints. Arch. Phys. Med. 31: 81-89, 1950.

11. Cnockaert, J.C., G. Lensel, and E. Pertuzon. Relative contribution of individual muscles to the isometric contraction of a muscular group. J Biomechanics 8: 191-197, 1975.

12. Cox, D.R., and H.D. Miller. The theory of Sochastic Processes. London: Methuen, 1965.

13. DeLuca, C.J.. Physiology and mathematics of myoelectric signals. IEEE Trans. on Biomed. Eng. 26(6): 313-325, 1979.

14. Glavinovic, M.I.. Presynaptic action of curare. J. Physiol. 290: 499-506, 1979.

15. Haffajee, D., N. Moritz, and G. Svantesson. Isometric knee extension strength as a function of joint angle, muscle length, and motor unit activity. Acta. Orthop. Scandinav. 43: 138-147, 1972.

16. Hallen, L.G., and O. Lindahl. Muscle function in knee extension - An EMG study. Acta. Orthop. Scandinav. 38: 434-444, 1967.

17. Henneman, E., G. Somjen, and D.O. Carpenter. Functional significance of cell size in spinal motorneurones. J. Physiol. 28: 566-580, 1965.

18. Johansen, S.H., M.J. Jorgensen, and S. Molbech. Effect of tubocurarine on respiratory and non-respiratory muscle power in man. J. Appl. Physiol. 19(5): 990-994, 1964.

19. Johnson, J.C.. Comparison of analysis techniques for electromyographic data. Aviat. Space Environ. Med. 49(1): 14-18, 1978.

20. Jorgensen, M., S. Molbech, and S.H. Johansen. Effect of decamethonium on head lift, handgrip, and respiratory muscle power in man. J. Appl. Physiol. 21(2): 509-512, 1966.

21. Joyce, G.C., P.M.H. Rack, and D.R. Westbury. The mechanical properties of cat soleus muscle during controlled lengthening and shortening movements. J. Physiol. 204: 461-474, 1969.

22. Kadefors, R., E. Kaiser, and I. Petersen. Dynamic spectrum analysis of myo-potentials with special reference to muscle fatigue. Electromyography 8: 39-74, 1968.

23. Komi, P.V., and J.H.T. Viitasalo. Signal Characteristics of EMG at different levels of muscle tension. Acta. Physiol Scandinav. 96: 267-276, 1976.

24. Knight, K.L. et al. EMG comparison of quadriceps femoris activity during knee extension and straight leg raises. Am. J. Phys. Med. 58(2): 57-69, 1979.

25. Kramer, H., G. Kuchler, and D. Brauer. Investigations of the potential distribution of activated skeletal muscles in man by means of surface electrodes. Electromyography 12: 19-27, 1972.

26. Lieb, F.J., and J. Perry. Quadriceps function - An Electromyographic study under isometric conditions. J. Bone and Joint Surg. 53-A(4): 749-758, 1971.

27. Lindahl, O., and A. Movin. The mechanics of extension of the knee-joint Acta. Orthop. Scandinav. 38: 226-234, 1967.

28. Lindstrom, L., R. Magnusson, and I. Petersen. Muscular fatigue and action potential conduction velocity changes studied with frequency analysis of EMG signals. Electromyography 10: 341-356, 1970.

29. Lippold, O.C.J.. The relation between integrated action potentials in human muscle and its isometric tension. J. Physiol. 117: 492-499, 1952.

30. Lloyd, A.J.. Surface electromyography during sustained isometric contractions. J. Appl. Physiol. 30(5): 713-718, 1971.

31. Lynn, P.A. et al. Influences of electrode geometry on bipolar recrdings of the surface electromyogram. Med. and Biol. Eng. And Comput. 16: 651-660, 1978.

32. Milner-Brown, H.S., and R.B. Stein. The relation between the surface electromyogram and muscular force. J. Physiol. 246: 549-569, 1975.

33. Milner-Brown, H.S., R.B. Stein, and R. Yemm. The orderly recruitment of human motor units during voluntary isometric contractions. J. Physiol. 230: 359-370, 1973a.

34. Milner-Brown, H.S., R.B. Stein, and R. Yemm. Changes in firing rate of human motor units during linearly changing voluntary contractions. J. Physiol. 230: 371-391, 1973b.

35. Molbech, S., and S.H. Johansen. Endurance time in static work during partial curarization. J. Appl. Physiol. 27(1): 44-48, 1969.

36. Mortimer, J.T., R. Magnusson, and I. Petersen. Conduction velocity in ischemic muscle: effect on EMG freqency spectrum. Am. J. Physiol. 219(5): 1324-1329, 1970.

37. Pengelly, L.D., et al. Effect of submaximal neuromuscular blockade on the ventilatory response to added mechanical loads to breathing. Study presented at Santorini, Greece, July 1977.

38. Pengelly, L.D., and J.R.A. Rigg. Effect of curare on the isometric contraction characteristics of tibialis anterior in the cat. Internal report. Departments of Medicine and Anaesthia, McMaster University, Hamilton, Ontario, 1978.

39. Pengelly, L.D., and J.R.A. Rigg. (unpublished data), 1979.

40. Rack, P.M.H., and D.R. Westbury. The effects of length and stimulus rate on tension in the isometric contraction of the cat soleus muscle. J. Physiol. 204: 443-460, 1969.

41. Ralston, H.J.. Uses and limitations of electromyography in the quantitative study of skeletal muscle function. Am. J. Orthodontics 47(7): 521-530, 1961.

42. Reilly, D.T., and M. Martens. Experimental analysis of the quadriceps muscle force and patello-femoral joint reaction force for various activities. Acta. Orthop. Scandinav. 43: 126-137, 1972.

43. Rigg, J.R.A.. Function of the diaphragm during partial neuromuscular block. Am. Rev. Resp. Dis. 119(2;2): 41-43, 1979.

44. Schweitzer, T.W. et al. Spectral analysis of human inspiratory diaphragmatic electromyograms. J. Appl. Physiol.: Resp. Env. Exer. Physiol. 46(1): 152-165, 1979.

45. Singleton, R.C.. On computing the Fast Fourier Transform. Comm. ACM. 10(10): 647-654, 1967.

46. Stulen, F.B., and C.J. DeLuca. The relation between the myoelectric signal and physiological properties of constant-force isometric contractions. Electroenceph. Clin. Neuro. 45: 681-698, 1978.

47. Wilkie, D.R.. The mechanical proprties of muscle. Brit. Med. Bull. 12: 177-182, 1956.

48. Zuniga, E.N., and Simons. Non-linear relationship between averaged electromyogram potential and muscle tension in normal subjects. Arch. Phys. Med. and Rehab. 613-620, Nov. 1969.